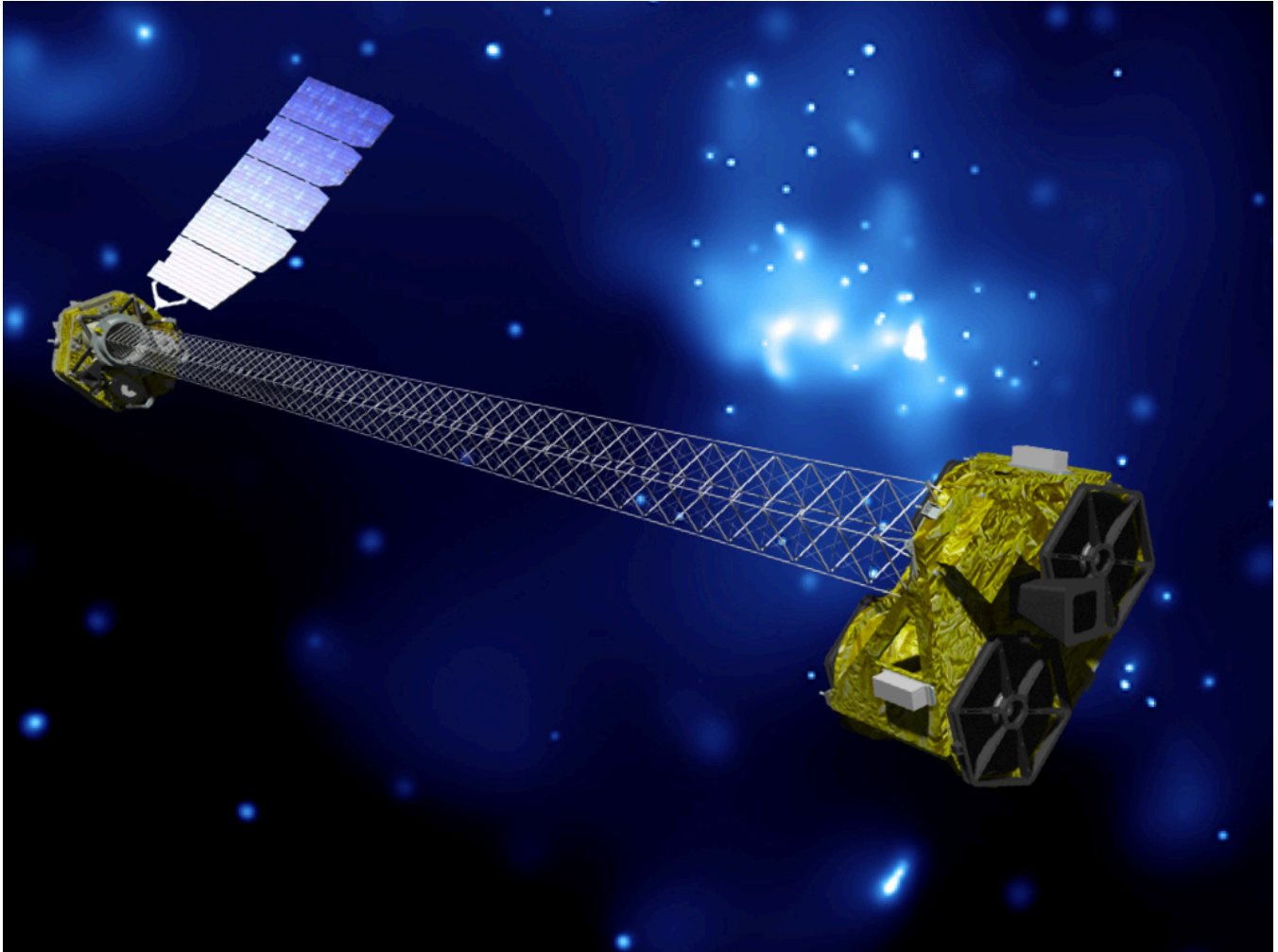*NuSTAR* Guest Observer Program

NuSTAR Observatory Guide

Version 1.0 (August 2014)

NuSTAR Science Operations Center, California Institute of Technology, Pasadena, CA

NASA Goddard Spaceflight Center, Greenbelt, MD

nustar.caltech.edu   heasarc.gsfc.nasa.gov/docs/nustar/index.html

Revision History

Revision	Date	Editor	Comments
D1,2,3	2014-08-01	*NuSTAR* SOC	Initial draft
1.0	2014-08-15		Release for AO-1

Table of Contents

List of Figures

List of tables

1. INTRODUCTION

The Nuclear Spectroscopic Telescope Array (*NuSTAR*) is the first focusing high energy (3-79 keV) X-ray space observatory. *NuSTAR* was launched on June 13, 2012 from the Reagan Test Site on the Kwajalein Atoll in the South Pacific in a compact, stowed configuration, on a Pegasus XL vehicle. First light was achieved on July 1st 2012 followed by a month of simultaneous calibration and science observations. Primary mission science operations began on August 1st 2012 and the observatory has a projected orbital lifetime of 10 to 15 years with no consumables. NASA has responded to the recommendation of the 2014 senior review of astrophysics missions by approving continued operations through 2016, including the implementation of a Guest Observer (GO) program with observations beginning in 2015.

This guide is intended to provide an overview of the *NuSTAR* observatory design, operations, and capabilities, and should help with a technical assessment for potential proposals solicited within the *NuSTAR* GO program. Information related to GO proposal tools and procedures can be found in section 4 of this guide and also on the *NuSTAR* GO website.

Sections 7, 8, & 9 in this document are for reference purposes and are not directly relevant for *NuSTAR* GO proposals.

Table 1 Additional information links

NuSTAR homepage	http://nustar.caltech.edu
NuSTAR GSFC website	http://nustar.gsfc.nasa.gov
NuSTAR SOC website	http://www.srl.caltech.edu/NuSTAR_Public/NuSTAROperationSite/Home.php
NuSTAR Guest Observer Program AO	http://heasarc.gsfc.nasa.gov/docs/nustar/nustar_prop.html
NuSTAR GO RPS page (requires RPS account)	https://heasarc.gsfc.nasa.gov/ark/nustar/
A description of the *NuSTAR* observatory and the primary science mission.	Harrison et al., (2013) ApJ 770, 103 (ADS)
NuSTAR in-orbit Calibration	Madsen et al., (2014)[2]
NuSTAR data analysis guide (NuSTARDAS)	http://heasarc.gsfc.nasa.gov/docs/nustar/analysis/nustar_swguide.pdf
NuSTAR public data archive	http://heasarc.gsfc.nasa.gov/docs/nustar/nustar_archive.html

Questions related to the *NuSTAR* GO program, data archive and analysis should be submitted through the HEASARC help desk

http://heasarc.gsfc.nasa.gov/cgi-bin/Feedback

Select NuSTAR under 'Choose a mailing list'.

1.1 *NuSTAR* Program Organization

NuSTAR is a NASA Small-class Explorer mission led by the California Institute of Technology (Caltech), which is responsible for the overall direction of the mission, with NASA's Jet Propulsion Laboratory providing project management. The *NuSTAR* Science Operations Center (SOC) is located at Caltech, with mission operations managed by UC Berkeley Space Sciences Laboratory. The *NuSTAR* Guest Observer Program is managed by NASA's Goddard Space Flight Center (GSFC) and all *NuSTAR* public science data, calibration files, and data analysis software, is made freely available through the HEASARC (see table 1). Major partners are the Danish Technical University Space Centre and the Agenzia Spaziale Italiana (ASI), which made significant contributions to hardware and data analysis software development. ASI is an active participant in mission operations, providing access to the Italian ground station at Malindi, Kenya.

2. THE *NUSTAR* OBSERVATORY

The *NuSTAR* observatory consists of two co-aligned hard X-ray telescopes pointed at celestial targets by a three axis stabilized spacecraft based on Orbital Science's LeoStar-2 bus which provides power, data handling, storage, and transmission, and attitude control (ACS) functions. Spacecraft attitude is determined using three star cameras developed by the Technical University of Denmark[3], mounted on the spacecraft bus.
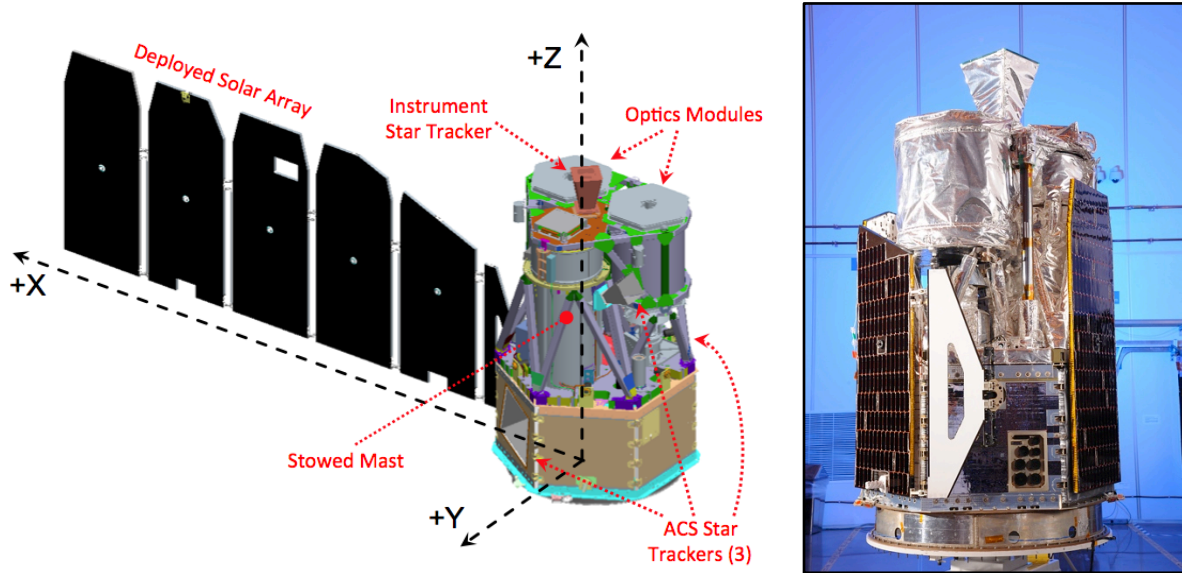
Figure 1 *Left* – Observatory configuration before on-orbit mast deployment. *Right* – Photograph of the observatory in the stowed configuration before launch.

In the fully deployed configuration the *NuSTAR* X-ray optics and detector benches are separated by a stiff mast that includes a mechanism with the capability of making small adjustments to optimize the location of the optical axis on the focal plane detectors. The X-ray optics bench consists of two co-aligned grazing incidence Wolter-I conical approximation[5] mirror modules, each with 133 shells coated with multiple layers of W/Si and Pt/C, limiting the highest efficient reflectivity to the Pt 78.4 keV K-edge [6,7,8]. The focal plane bench is mounted on the spacecraft bus and consists of two independent solid state photon counting detector modules (FPMA & B), each with a 2x2 array of CdZnTe (CZT) crystal detectors, surrounded by CsI anti-coincidence shielding. The detectors are passively cooled and operate at 15°C [9,10].

Figure 2 *Left* - Photographs of one of the two optics modules. Each mirror assembly has 133 shells. *Right* - One of the two detector modules with 4 CZT detector crystals. Each detector crystal measures 2cm x 2cm and contains an array of 32x32 independently discriminated pixels.
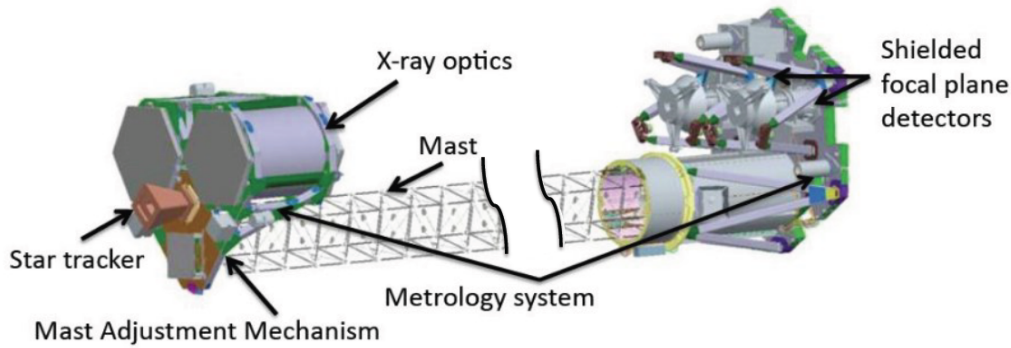
Figure 3 Design of the *NuSTAR* telescopes, the length of the mast is not to scale.

The *NuSTAR* telescope design is unique, with the optics held 10.14m from the detectors using a lightweight carbon-fiber/titanium extendable mast based on a redesign of the extendable mast used in the Shuttle radar topography mission, STRM[4]. The mast is stiff but the orbital motion through cycles of Earth shadow and Sunlight results in displacements of the optics focal point on the detector bench on the order of 1 – 3 mm. This relative motion of the two benches with respect to each other is accurately tracked by a laser metrology system which measures the translation, tip, tilt and clocking between the benches down to a few microns. The *NuSTAR* observatory also operates an aspect alignment system that consists of a star camera mounted on the optics bench to provide an absolute celestial reference, and combined with the metrology data, enables accurate image reconstruction of celestial X-ray sources.
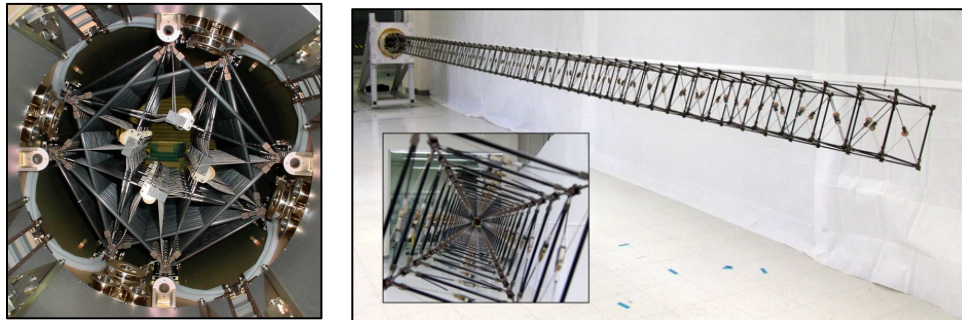
Figure 4 *NuSTAR* deployable mast, Left - stowed in canister. Right - Deployment test before integration with spacecraft.

NuSTAR was designed such that one side of the observatory always faces the Sun, and pointing to a celestial target is achieved by rotating the observatory about the Sun-Earth vector. This allows the use of a solar array with a single axis of rotation and simplifies the thermal design. The observatory is designed for long observations, typically 1 day to weeks in duration, and does not re-orient during periods of Earth occultation.

2.1 *NuSTAR* Performance

The *NuSTAR* observatory was calibrated during the first few months of operations, making a series of observations of celestial sources for performance verification, as well as internal calibration using a deployable [155]Eu source, and cross-calibration with other missions. The primary calibration source in orbit is the Crab and information about observatory instrumentation is given in section 3 with details on the in-flight calibration in Madsen et al. (2014)[2]. The resulting performance of the observatory is given below in table 2.

Table 2 *NuSTAR* observatory performance parameters

Spacecraft		Telescopes (2 modules)	
Launch (Orbital Pegasus)	June 13, 2012	Focal length	1014 cm
Bus	Orbital LeoStar-2	Field of view	12.2 x 12.2 arcmin
ACS	3x DTU Star trackers	Angular resolution	58″ HPD 18″FWHM
Mass	350 kg	Aspect reconstruction (bright source)	1.5″ (1σ)
Power	600 W	Absolute astrometry	8″
Orbit	(2014)	Focal plane CdZnTe detectors (2x2 array/module)	
Inclination	6 degrees	Size	2 x 2 cm
Altitude	610 to 650 km	Physical pixel number	32 x 32
Period	97.126 minutes	Pixel pitch	604.8 μm
Ground station	Malindi (ASI), Kenya	Sky plate scale	2.45 arcsec
		Maximum readout rate	400 events s^{-1}
Operations		Energy range	3 to 78.4 keV
Sun / Full-Moon avoidance*	> 50 / 14 degrees	Spectral resolution	400 / 900 eV at 10 / 68 keV
Slew rate	0.06 degrees s^{-1}	Temporal resolution	2 x 10^{-3} s (RMS)
ToO response time	< 24 hours		
Settling time (typical)	200 s	*NuSTAR is designed to be able to observe the Sun	
Sensitivity	(10^6 s, 3σ, ΔE/E = 0.5)	Background in HPD	
6-10 keV	2 x 10^{-15} erg cm^{-2} s^{-1}	10 – 30 keV	1.1 x 10^{-3} counts s^{-1}
10-30 keV	1 x 10^{-14} erg cm^{-2} s^{-1}	30 – 60 keV	8.4 x 10^{-4} counts s^{-1}
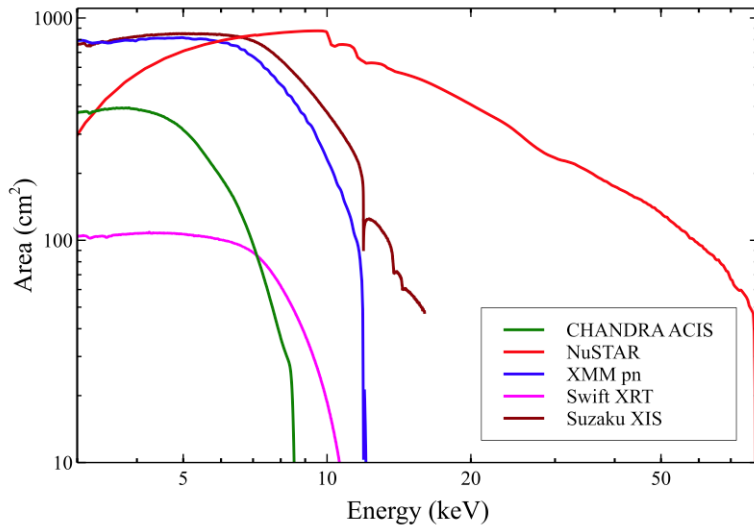
Figure 5 Effective collecting area of *NuSTAR* compared to selected operating X-ray focusing telescopes. *NuSTAR* provides good overlap with these soft X-ray observatories and extends focusing capabilities up to 79 keV

2.2 Primary mission science observations

The *NuSTAR* primary mission science working groups for the 2-year *NuSTAR* baseline mission have guided the target selection and provided the SOC with information about target positions, expected count rates, and scheduling constraints. An up-to-date list of publications based on *NuSTAR* observations can be found on the *NuSTAR* homepage (http://www.nustar.caltech.edu/page/publications). Approximately 50% of the available observing time was made available to conduct surveys of large areas of the sky:

- Galactic center and plane, including Sgr A*.
- Extragalactic surveys in the COSMOS, ECDFS, & GROTH fields.
- Short exposures of a large sample (>200) of active galaxies chosen from the *Swift*-BAT 70-month catalog[12].

This last survey group is very helpful in improving the overall observing efficiency of the mission as the short exposures can be scheduled to break up long (>40 minute) slews between targets that have scheduling constraints. It may also be possible to use data taken during the slews between targets because the instrument remains active during slews. However it is unlikely that a slew-survey will detect new sources because the average exposure time at any point on the sky during a slew is ~3 seconds.

A list of observations that are scheduled to be carried out as part of the *NuSTAR* team investigations and legacy survey programs can be found on the *NuSTAR* website at:

http://www.nustar.caltech.edu/page/researchers

and are also available within the numaster catalog hosted by the *NuSTAR* Archive at HEASARC

http://heasarc.gsfc.nasa.gov/W3Browse/nustar/numaster.html

3. INSTRUMENTATION

3.1 Calibration

Extensive calibration of the instrument and modeling of the X-ray optics were performed prior to launch and details of the in-orbit refinement and re-calibration of the *NuSTAR* observatory is presented in Madsen et al. (2014)[2]. The Crab nebula is primary calibration target for almost all space X-ray observatories and was also used by *NuSTAR* for calibration of the effective area, event timing, and vignetting of the telescope. Additional observations of various astrophysical X-ray sources have also been made and table 3 gives a summary of the in-orbit calibration activities during the first two years of operations.

Table 3 *NuSTAR* observatory in-orbit calibration activities

Aspect alignment		
Cyg X-1	July 2, 2012	Cyg X-1 was the observatory first light target. Subsequent aspect
Bright targets	July 2012	alignment during IOC used multiple bright X-ray celestial sources
Effective Area		Calibration assumes canonical Crab spectrum
Crab	Sept 2012 to Nov 2013	Crab observed in 39 short exposures at various positions on the focal plane.
Gain and energy resolution		
Onboard ^{155}Eu source	June 24, 2012	Deployed only once in each focal plane for initial gain calibration refinement
Cas A, Tycho SNR	Aug 2012 – 2014	Emission line measurements from multiple observations can track gain
Internal background lines	ongoing	changes.
Cross calibration with other observatories		
3C 273	July 14, 2012	Cross calibration with *Chandra*, *XMM-Newton, Swift, Suzaku, & INTEGRAL*
Crab, PKS 2155-304	2013-2014	Yearly coordination with *Chandra*, *XMM-Newton, Swift, & Suzaku*
Point Spread Function		PSF is strongly peaked, HPD decreases slightly (~few%) with increasing energy.
Cyg X-1	2012-2013	No change in PSF FWHM with off-axis angle but distorts azimuthally
Bright targets, e.g. Vela X-1, Her X-1		No significant change in PSF over the first year of the mission.
Timing		
Crab pulsar	2012-2013	Compared to radio telescope pulse measurements
PSR B1509-58	Aug 2013	Compared to *Swift*-XRT simultaneous timing measurements
Background		
Extragalactic surveys	ongoing	Identification of scattered Solar X-rays when satellite is in daylight
Earth occultation periods	ongoing	Identification of scattered cosmic X-ray background

Many of the calibration targets are also science targets for the mission so the total time specifically dedicated to calibration observations since science operations began in August 2012 is less then 1%. This is not anticipated to change during the extended mission and the primary calibration activity will be the cross-calibration campaigns with other observatories coordinated through IACHEC[14]. *NuSTAR* became an active member of IACHEC before launch and the support of the community for early cross calibration observations was greatly appreciated by the *NuSTAR* team. The yearly IACHEC meetings provide a forum to discuss calibration activities and have improved communication between the observatory operations teams. The absolute normalization of the *NuSTAR* effective area was adjusted in 2013 based on the cross calibration campaigns of 2012 and 2013 and measurements are seen to agree to within 15% between concurrent X-ray observatories with widely differing design, capabilities, and bandpass[29].

3.2 Optics

NuSTAR flies two identically designed conical Wolter-I approximation optics called OMA (Optics Module) and OMB. OMA is matched with the Focal Plane Module, FPMA, and OMB with FPMB. Each optic is composed of 133 mirror shells; the outer 43 shells are coated with a W/Si multilayer while the inner 90 shells are coated with Pt/C, limiting the

highest efficient reflectivity at the Pt 78.4 keV K-edge. The focal length is 10.14 meters for an effective plate scale at the focal plane of 20.34″ mm⁻¹.

3.2.1 Effective area

The effective area of the mirrors was calibrated using the Crab. The phase-averaged integrated spectrum of the nebula and pulsar was assumed to be an absorbed power-law of Γ = 2.1, normalization at 1 keV of N = 8.5 ph keV⁻¹ cm⁻² s⁻¹, and hydrogen column N_H = 2.2 x 10²¹ cm⁻². The reasons for choosing the spectrum and N_H can be found in Madsen et al. (2014)[2]. The effective are has been reliably calibration between 3 – 78 keV. The Pt K-edge is located at 78.4 keV, but it was not possible to reliably correct this edge due to an insufficient data set, and fitting up to this energy has a high likelihood of producing residuals. Remaining residuals at the W k-edge at 69.5 keV may also still be evident if the source is strong enough.

Because of the mast, which cycles through sunlight and shadow once during each orbit, the optical axis (OA), moves across the focal plane in a cyclical pattern. Since the OA track and source track are not the strictly coupled, the source will experience a range of off-axis angles with typically variations of 30″-60″. Additionally, because of detector gaps, the aimpoint of the target is offset by about 1′ from the OA location, and so typically an 'on-axis' observation is taken at an off-axis angle of around 1′–2′.

Figure 6 shows the effective area of 1′, 3′ and 5′ of FPMA (one module) assuming an infinite focal plane (i.e. without PSF losses) and the residuals for all Crab observations within 3′. The residuals are better than +/-2% up to ~40 keV. Between 40 – 80 keV, residuals are dominated by counting statistics of the Crab data, but are typically 5 – 10%, so the systematic errors are less than that. The scatter in flux is 2-3% (1 sigma). Because the knowledge of the optical axis is about ~30″, it is not uncommon to see flux differences between module A and module B of up to 5% within an observation.

For more details on the effective area calibration see Madsen et al., (2014)[2].
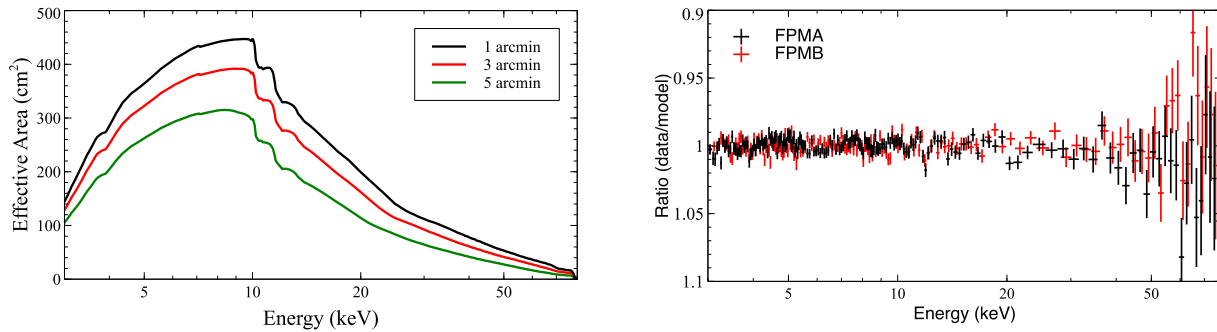
Figure 6 *Left* – Dependence of effective area for one telescope with energy and off-axis angle. *Right* - Residuals to model fit of Crab observations.

3.2.2 Point Spread Function

The shape of the *NuSTAR* Point Spread Function (PSF) was derived using a physics based ray-trace model and an empirical modification function. Figure 7 shows images of the two PSF from OMA and OMB using a logarithmic scale and stretched to highlight faint features. The visible structures are caused by support spiders and gaps in the glass between sections, but apart from these there are no significant artifacts or asymmetries. The shape of the PSF is centrally sharp, with extended wings. The PSF has a slight energy dependency and shrinks with increasing energy as shown in Figure 8. Table 4 summarizes the Half Power Diameters as a function of energy.

Table 4 Half Power Diameters as a function of energy for the *NuSTAR* modules. Errors are of order 1″.

Energy (keV)	FPMA HPD (″)	FPMB HPD (″)
3 − 4.5	70.3	65.6
4.5 − 6	67.1	62.6
6 − 8	64.7	60.7
8 − 12	63.5	59.5
12 − 20	63.4	60.3
20 − 79	63.4	62.4
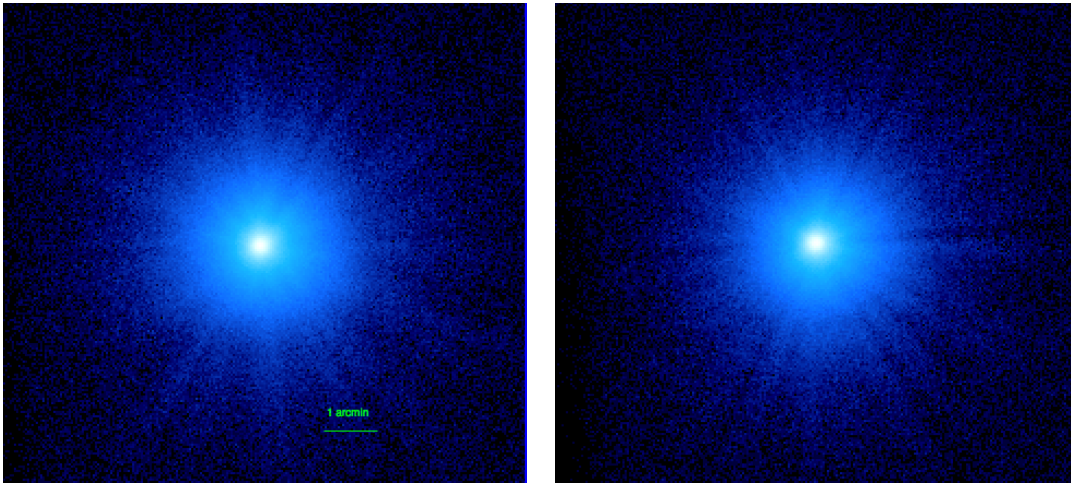
Figure 7 Stretched images of the *NuSTAR* PSF for FPMA (*left*) and FPMB (*right*).
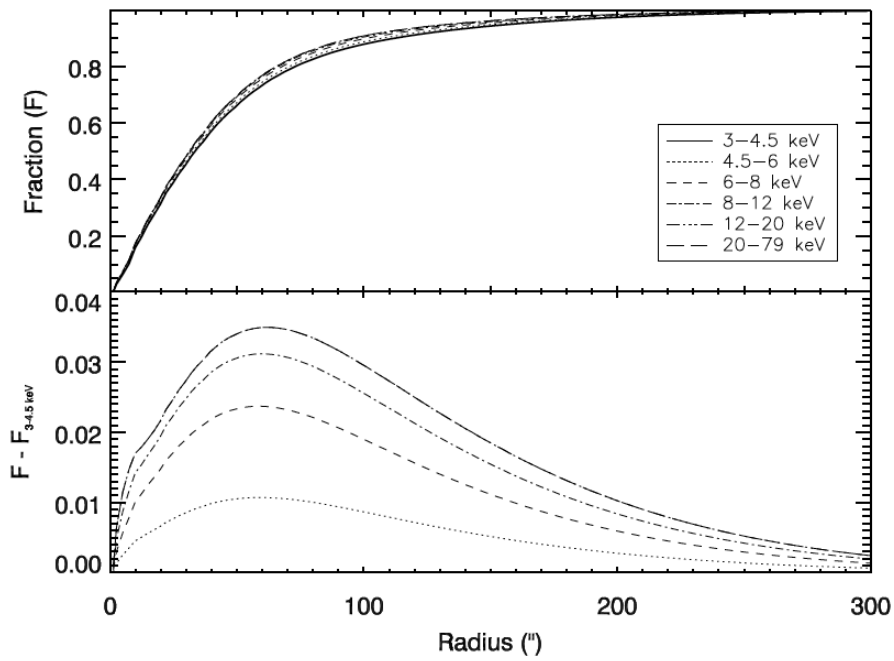
Figure 8 Energy dependency of *NuSTAR* PSF.

3.3 Detectors

The detector modules are composed of four 2 mm thick CdZnTe crystals hybrid pixel detectors, resulting in a focal plane of 4 × 4 cm, which at a focal length of 10.14 m covers a Field of View (FoV) of 12.45 arcminutes. Each crystal has 32 × 32 (= 1024) pixels, subdivided in software by a factor of 5 to an imaging sampling of 2.45 arcsecond. The focal planes are passively cooled to 3 and 5° C (FPMA/B respectively). Since launch, both modules have been stable and the performance has been better than requirements. Details on the calibration and in-orbit performance of FPMA and FPMB can be found in Kitaguchi et al., (2011, 2014)[14,15].

3.3.1 Detector performance stability

There has been no measureable decline in the sensitivity of the CZT detectors during the first two years of on-orbit operations. The detectors have remained stable on orbit, with no need to automatically search for and disable noisy pixels every orbit as planned before launch. As of August 2014 more than 99.6% of all detector pixels remain active. The only change to the detectors during nominal science operations has been an adjustment of the anti-coincidence shield thresholds on 2014-06-12.
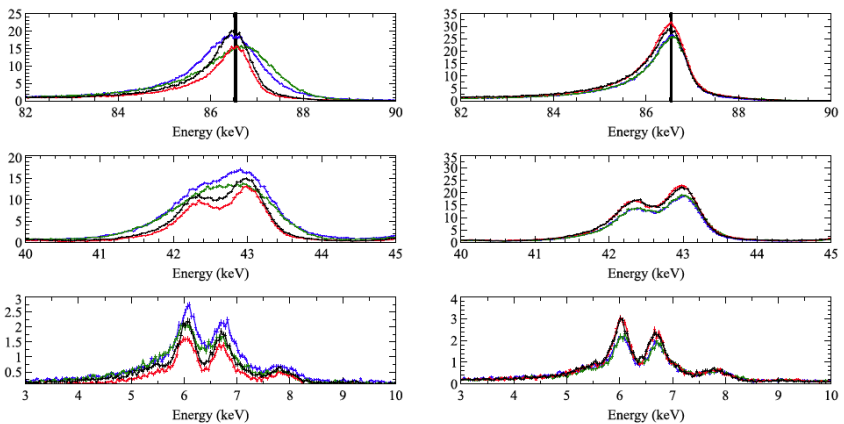
Figure 9 Spectrum of the calibration source for FPMA (*left*) and FPMB (*right*) after all gain corrections have been applied. Three regions are displayed centered about prominent emission lines from the ^{155}Eu calibration source.

3.3.2 Detector gain

The instrument calibration source is primarily composed of the radioisotope Eu-155 and can illuminate all pixels on both focal planes. The calibration source has several prominent lines at high energies (86.54 and 105.4 keV) and low energies (6.06 and 6.71 keV) that are used to confirm the gain of the instrument.

Figure 9 shows the lines of the calibration spectrum. The error on the absolute energy scale is typically 10 to 20 eV for all grade combinations, less than half a *NuSTAR* channel width (PI), while the detector gains are typically accurate to a statistical uncertainty of one part in 100,000. The one exception is for DET2 on FPMA, which appears to have small non-linearity in the gain response at high (>80 keV) energies while the energy response across the *NuSTAR* science band (3--79 keV) appears to be consistent with the other detectors.

3.3.3 Instrument dead time

NuSTAR observations of bright X-ray sources do not suffer from the effects of pileup inherent to CCD detectors like those flown on soft X-ray observatories (*Chandra*, *XMM-Newton, Swift*). However, a fraction of photons incident on the *NuSTAR* CZT detectors are not recorded. The instrument dead time results from the electronics not accepting events due to shield veto signals, preamplifier reset, and the time required for the MISC to process events. The dead time fraction at a particular measured count rate can be expressed as

$$DTF = [s(1-c)(1-eR) + c(1-s)(1-eR) + eR(1-s)(1-c)]$$

where *s* is the shield veto fraction, *c* is the charge pump reset fraction, *e* is the per event processing time, and *R* is the count rate in Hz in an individual telescope.

Y-axis: Observed count rate (0, 50, 100, 150, 200, 250, 300, 350, 400)
X-axis: Incident count rate (10.0, 100.0, 1,000.0, 10,000.0, 100,000.0)
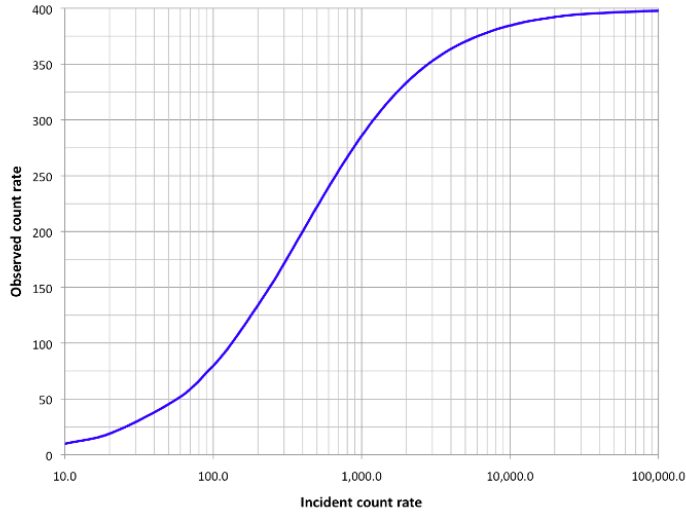
Figure 10 Relation between the observed count rate and the incident count rate for a *NuSTAR* focal plane consisting of 4 detectors. The expression breaks down at very high count rates, $> 10^5$ s^{-1}.

Table 5 Observed count rate (R_o) as a function of incident count rate (R_i)

R_o	20	50	75	100	150	180	200	220	240
R_i	21	57	92	133	240	327	400	489	600
R_o	250	260	270	280	290	300	310	320	330
R_i	667	743	831	933	1055	1200	1378	1600	1886
R_o	340	350	360	370	380	385	390	395	399
R_i	2267	2800	3600	4933	7600	10267	15600	31600	159600

Note that fluxes can be measured even for sources with count rates high enough to result in 100% dead time. The electronics are configured such that the time interval from the end of event processing to the next event trigger is accurately measured. This is done to an accuracy of 1 microsecond. So if the focal plane is illuminated with 10,000 cps the flux can still be measured to 1%, even though only 400 events s^{-1} will be processed.

The exposure time is automatically corrected for dead time, and thus if a target was observed for 4000 s with a dead time of 50% then the final effective exposure time is 2000 s.

3.4 Ghost Rays and Stray Light

The *NuSTAR* mirror design is based on the Wolter-I conical approximation, which is a double mirror design that focuses X-rays with two grazing angle reflections. It is possible for photons at very shallow or very steep angles to be reflected only once by the mirror assembly. These 'Ghost Rays' can originate from sources between 3′ and 40′ off-axis and are readily apparent for bright sources at these angles. Analysis of off-axis sources includes a correction, performed within the NuSTARDAS (see section 5), that adjusts the effective area by <5% for energies below 60 keV[29].

There can also be an additional component in *NuSTAR* images that is due to unfocussed light from bright sources between 3° and 6° off-axis, i.e. well outside the field of view (12′ across). This 'Stray Light' is from the part of the sky that is not blocked by the telescope aperture stops or the optics bench (see Figure 11). Although the two telescopes on *NuSTAR* are co-aligned and the aperture stops will block any flux from the sky at > 6° off-axis, the part of the sky blocked by the optics bench is different for the two focal plane detectors, and so the Stray Light pattern can appear different for each detector and will vary with the position angle of the observation.

In the example shown in Figure 11 rays from the source are shielded from striking the left detector plane by the optics bench, but the other rays from the same source have an unimpeded path through the aperture stop to shine on a corner of the right detector plane.
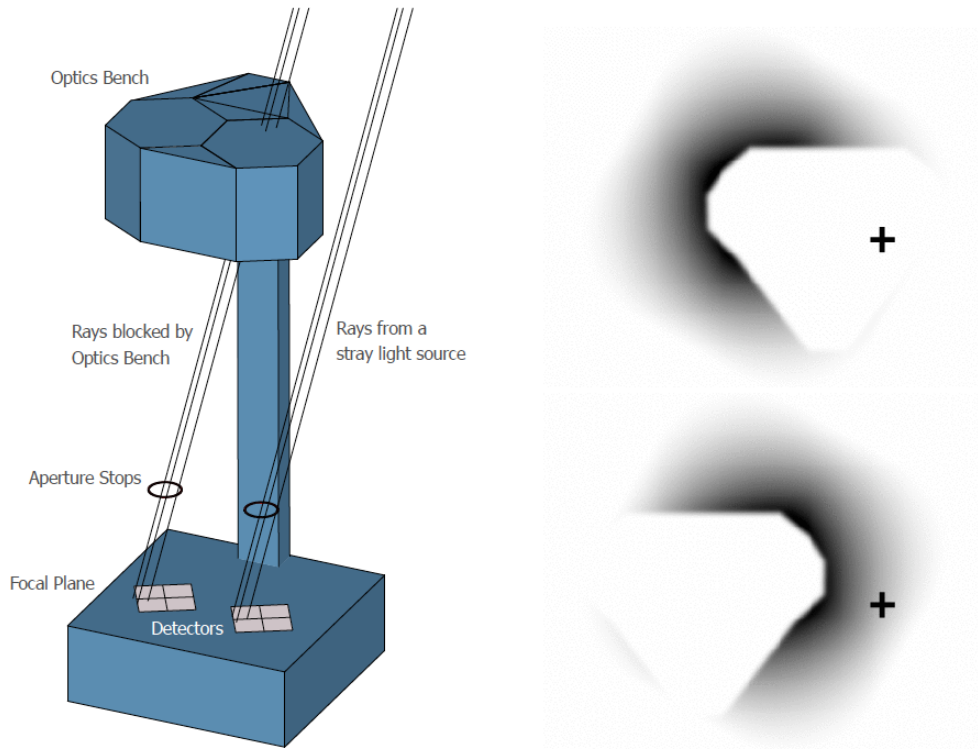
Figure 11 *Left* – Schematic of the observatory that illustrates how far off-axis sources can directly shine on the detectors through the aperture stop, producing the Stray Light background. *Right* – The location of sources on the sky, as visible from the detector plane, that produce the Stray Light background for FPMA (*top*) and FPMB (*lower*). The images are weighted (darker) by the number of detector pixels a given source shines on. The crosses give the approximate position of the source shown in the left panel. From Wik et al., (2014)[13].
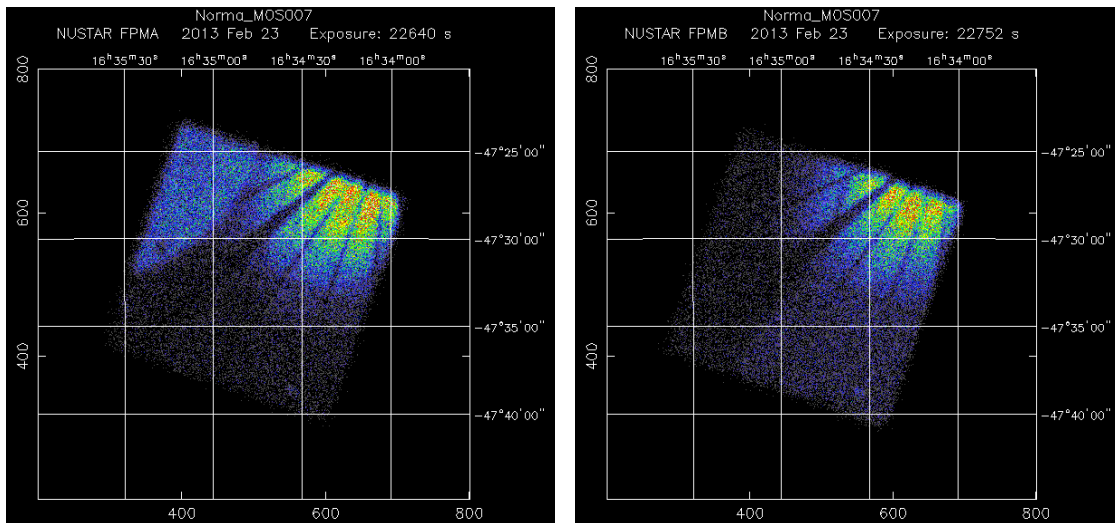
Figure 12 Example Ghost Ray and Stray Light patterns from sources outside *NuSTAR* field of view from part of the Norma region survey (ObsID 40014001001). Sky image from FPMA (North is up, East is to the left). A Ghost Ray petal-like pattern from the bright X-ray source 4U 1630-47 located 11.8 arcmin from the center of the field of view to the NW is evident in both focal plane images. Stray Light is also present in the NE of the FPMA image (*left*) and covering the SW corner of the FPMB image (*right*).

Planning observations in areas of the sky crowded with bright X-ray sources has to consider the possibility of Stray Light contaminating the observation and this leads to a scheduling constraint when only small ranges of PA are optimal.

3.5 Instrument Background

The low inclination of the *NuSTAR* orbit was chosen to keep the instrument background low and stable by only skirting the Northern edge of the South Atlantic Anomaly (SAA). Compared to previous missions with instruments operating in the hard X-ray region the *NuSTAR* background is very low, < 1 event/s for each telescope and for observations over many orbits the variations in background average out, leaving uncertainties of < 1%. The spectrum of the *NuSTAR* instrument background is well understood and a detailed investigation is presented in Wik et al. (2014)[13].

The major contributions to the observatory background are presented in Figure 13 and can be characterized as originating from:

- Instrument Compton scattered continuum emission (*Int. Cont.*).
- Instrument emission lines (*Int. Lines*).
- Cosmic X-ray background from the sky leaking past the aperture stops (*Aperture*).
- Reflected Solar X-rays (*Solar*).
- Focused and Ghost Ray Cosmic X-ray background (*fCXB*).
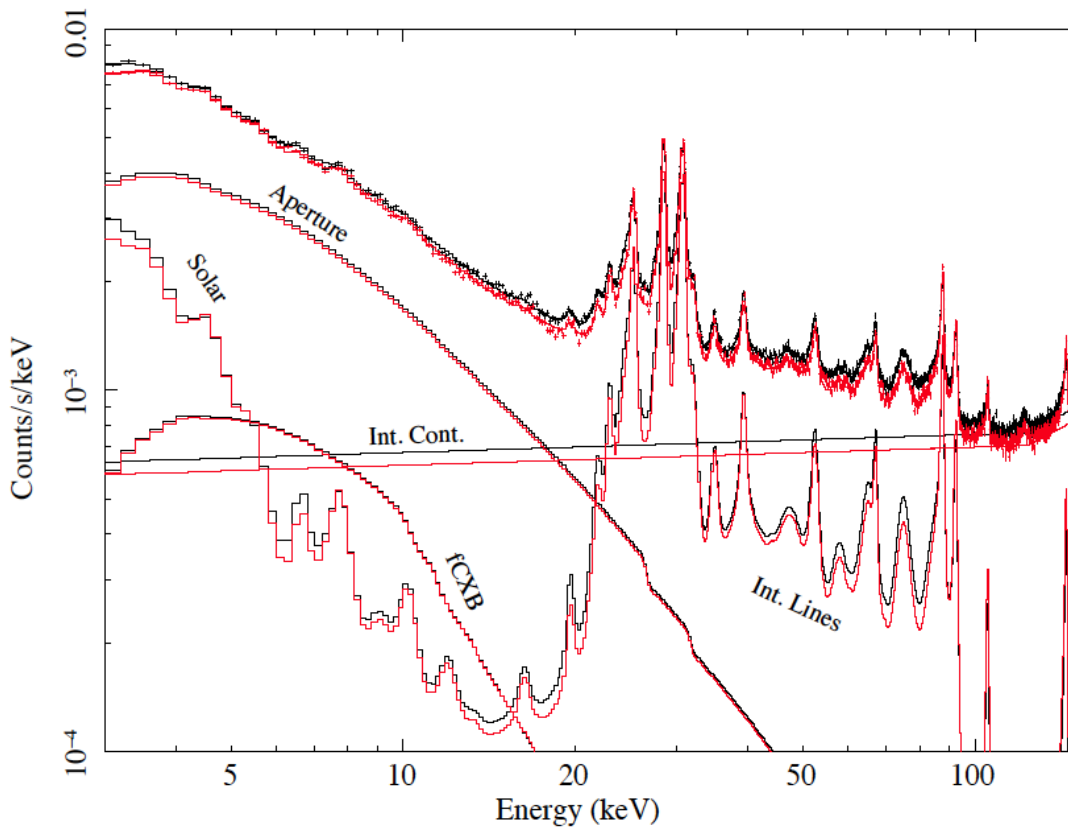
Figure 13 Components of the *NuSTAR* observatory background spectrum, from Wik et al., (2014)[13]. The spectrum represents the rate in each focal plane module (A=black, B=red). Each detector has an approximate area of 400 cm^2 and covers approximately 36 arcmin^2 solid angle.

These components produce a spatially non-uniform and time varying background in all *NuSTAR* observations but this is only of particular concern for investigations of diffuse (e.g. galaxy clusters) and/or faint sources (e.g. sky survey programs).

12

3.6 Timing Calibration

The X-ray event timing is kept stable to within a few milliseconds by correcting the drift of the spacecraft clock relative to UT clocks at the ground stations with additional corrections performed at the SOC. Corrections to the spacecraft clock are applied to during ground station passes if the drifts are larger then ±10 msec from true time, see Roberts et al. (2014)[11]. The track of the clock adjustments is provided by the MOC and an interactive tool is used to calculate spline interpolation between the spacecraft clock corrections to keep the relative timing accuracy to within ±2 msec. These corrections are recorded in a clock correction calibration file, distributed within the *NuSTAR* CALDB, which can be used within NuSTARDAS and the general-purpose FTOOL barycorr to correct event times to the equivalent Solar System barycenter.

The timing accuracy of *NuSTAR* events was investigated using the Crab pulsar calibration data and indicates an overall accuracy in relative timing of ±3 msec. The absolute accuracy of event times was also confirmed using observations of the pulsar PSR B1509-58 and is found to be 1 ±2 msec compared to measurements by *Swift*-XRT[2].

The frequency of the *NuSTAR* spacecraft clock is expected to depend on the temperature of the crystal oscillator. Although the spacecraft clock uses a temperature compensated crystal oscillator there appears to be some residual drifts that scale linearly with the temperature of the clock housing (~0.4 ppm over the 6 °C observed temperature range).

There has been no sign of any degradation in the performance of the spacecraft clock oscillator on-orbit.

4. GUEST OBSERVER PROGRAM

The response of the 2014 NASA Senior review to the proposed extension of *NuSTAR* operations past the primary mission was very positive; *NuSTAR* was ranked second out of the nine missions reviewed, and NASA has directed the project to implement a Guest Observer (GO) program with observations beginning in 2015. Details of the *NuSTAR* GO solicitation are available through the NASA Solicitation and Proposal Integrated Review and Evaluation System (NSPIRES, http://nspires.nasaprs.com/external/) and the *NuSTAR* GO website at HEASARC (http://nustar.gsfc.nasa.gov/docs/nustar/nustar_prop.html) including key dates for the GO program.

The GO program is a component of the approved *NuSTAR* mission extension plan which has the following key components:

Table 6 Key components of *NuSTAR* extended mission

Program element	Time Fraction	Available Exposure Time (Msec)	Implementation / Data Policy
Guest Observer Program	50%	8.50	Open call for proposals each year. Time also offered through *XMM-Newton* and *Chandra* AOs. 12 month limited use period.
Legacy surveys	25%	4.25	Planned by science team with community input. Data released after 60 day validation period. High level catalogs and transient alerts provided by he SOC.
PI Discretionary time	15%	2.55	Unanticipated ToOs open to the community to request. 6 month limited use period for the proposer.
Program Reserve	10%	1.70	Reserve for calibration, engineering and unanticipated operational issues. Calibration data has no limited use period.

Details for *NuSTAR* Cycle 1   (2015-04-01 to 2016-03-31)

NuSTAR		6.50	Joint *Suzaku* program can be proposed in *NuSTAR* AO1 Up to 0.5 Msec of *Suzaku* exposure time available
XMM-Newton		1.50	Joint programs solicited through the *XMM-Newton* AO14
Chandra		0.50	Joint programs solicited through the *Chandra* AO17

The *NuSTAR* legacy surveys represent extensions of the baseline mission Galactic and extragalactic surveys. The legacy survey data will be immediately made public, and source catalogs and spectra will be released as soon as they have been processed. During the baseline mission, the remainder of the field of view for a specific target, including optical follow-up observations when available, were used to create a wide-area serendipitous source survey. This practice will be continued in the GO phase, with the inclusion of non-target background sources in the legacy surveys. However, the GO will retain data rights to any background source in the field of his/her primary target that is of interest beyond contributing to the wide-area survey statistics for the duration of the exclusive-use period.

The *NuSTAR* GO program organization takes advantage of the extensive HEASARC experience with similar GO programs for other explorer missions. The HEASARC will manage the GO proposal review process with appropriate oversight from NASA headquarters. Proposals should be submitted using the *NuSTAR* entry in ARK/RPS tool and the *NuSTAR* SOC will be responsible for technical review of proposals after the proposal deadline.

4.1 GO Program Technical Limitations

There are a number of specific technical limitations for *NuSTAR* GO proposals for which online tools are available to aid in the evaluation of proposal requests. See section 4.3 for a list of tools available for determination of observation parameters and section 4.5 for examples of observation simulations. Proposers should pay special attention to the following technical issues for *NuSTAR* observations:

1. The requested **exposure time** per observation (i.e., a single "visit" to a target) must be between a minimum of 20 ksec and a maximum of 500 ksec.

The low inclination (6°), low altitude (~600 km) orbit of *NuSTAR* allows on average only 3.2 ksec continuous exposures per 95 minute satellite orbit for targets with declination ≤ |65°|. Guest observers should request exposure times necessary for achievement of the proposed science goals, excluding observational efficiency factors (Earth occultations and South Atlantic Anomaly passages, see section 8) in the calculations, unless there is a specific reason why the elapsed time of an

observation is important. For targets with high declination, (> 65°), the unocculted period may be longer; however, specification of elapsed time requirements will result in the observation being classified as time-constrained.

2. **Time constrained** observations are defined as an observation that must be performed within a specific time window, i.e.
   a. must occur at a specific date/time or with a specific duration (e.g. for minimum of 10 hours real time duration).
   b. must occur at a specific phase in the targets' ephemeris.
   c. are designed to monitor a target with more then one visit (minimum separation between visits is 14 hours).
   d. must be performed at a specific observatory position angle.

Proposers are referred to the specific instructions in the latest GO program cycle AO to review the restrictions on acceptance of time constrained observations.

3. **Coordinated observations** for joint *Suzaku*/*NuSTAR* programs will be accepted contingent on the continued health of the *Suzaku* observatory up to a total of 500 ksec of *Suzaku* observing time.
   a. Proposals for coordinated observations will be designated as time constrained.

Cycle 1	Proposals for coordinated observations with the *Chandra* and/or *XMM-Newton* observatories are NOT solicited by the *NuSTAR* GO program. Individuals wishing to request coordinated observations with these observatories should respond to the *Chandra* Cycle 17 or *XMM-Newton* Cycle 14 solicitations.

4. **Bright sources** are defined as any target that has a predicted instrument count rate of ≥ 100 counts s^{-1} for both modules using a 50% extraction with no dead time (see section 3.3.3).
   a. See section 4.5 for instructions on how to estimate the *NuSTAR* count rate.

Transmission of the data during observations of bright targets require the scheduling of additional ground station contacts to avoid the risk of overwriting on-board data. The resources allocated to operating a SMEX mission place a limit on the number of ground station passes that can be allocated.

Cycle 1	The total observing time in the GO cycle that can be allocated to bright targets is limited to ~200 ksec.

5. Targets should be evaluated for the potential impact of **Stray Light** during an observation (see section 3.4).
   a. Sources with fluxes $> 10^{-11}$ ergs s^{-1} cm^{-2} within 5° of the target may cause increased non-uniform background gradients due to Stray Light.
   b. Users should check observations for potential Stray Light contributions using the tools available at http://nustar.caltech.edu/page/researchers.

If a field is designated as 'heavily contaminated', proposers should submit a request for a feasibility analysis to nustar-help@srl.caltech.edu at least two weeks prior to the proposal submission deadline.

6. Proposals for **Target of Opportunity** (ToO) observations are NOT solicited through the GO program.
   a. Information for requesting ToO or directors discretionary time can be found at http://www.nustar.caltech.edu/page/too_policy
   b. Data from ToO observations will have a six-month exclusive-use period.

4.2 *NuSTAR* Proposal Details

NuSTAR GO program details can be found on the *NuSTAR* HEASARC website:

> http://heasarc.gsfc.nasa.gov/docs/nustar/nustar_prop.html

including a proposal thread that can be used as a guide to the proposal submission process.

4.3 Proposal Tools

Online tools are available for proposers that will provide an estimate of the exposure time and the impact of Stray Light for a *NuSTAR* observation.

SOC target constraint check
• Sun, Moon, Star Tracker constraints • Position Angle determination for observation date • Preliminary Stray Light evaluation
URL: http://www.srl.caltech.edu/NuSTAR_Public/NuSTAROperationSite/CheckConstraint.php
Notes: Based on target J2000 coordinates, default evaluation is for 1-year GO cycle. Output will indicate if there is a possibility of heavy contamination of the field of view by Stray Light.
RPS input: Stray Light information should be included in the ARK/RPS form for each proposed target(s).

WebPIMMS
• Target count rate • Convert from model and flux to *NuSTAR* count rate • Convert from mission (e.g. *Chandra*, ASCA, etc.) count rate to *NuSTAR* count rate
URL: http://heasarc.gsfc.nasa.gov/cgi-bin/Tools/w3pimms/w3pimms.pl
Notes: Multi-mission count rate simulator, has multiple spectral component model interface available.
RPS input: Input PIMMS prediction of *NuSTAR* count rate for both modules for a 50% PSF extraction without accounting for dead time.

WebSpec
• Web interface for XSPEC • Simulates spectral data for multiple missions • Convert from spectral model and count rate to simulated spectrum
URL: http://heasarc.gsfc.nasa.gov/webspec/webspec.html
Notes: Do not include pileup. Default is the 50% PSF extraction but 80% PSF extraction region is also available.
RPS input: Useful for evaluation of expected significance of spectral component parameter measurement.

Archive *NuSTAR* master catalog (*numaster*)
• BROWSE and XAMIN interface to *NuSTAR* archive tables • numaster catalog contains a list of *NuSTAR* observations which have been processed and successfully validated by the SOC • Data from these observations may or may not be public • Information for planned (and unobserved) targets is also available in the numaster catalog (status=accepted). • ToO observations will most often first appear in the numaster catalog with status=observed. • DDT targets may be added to the numaster catalog with status=accepted or status=observed depending on the time between the acceptance/observation of the target and the timing of the numaster catalog updates.
URL: http://heasarc.gsfc.nasa.gov/cgi-bin/W3Browse/w3browse.pl
Notes: Check the public_date parameter to determine if the data is publically available. Unobserved targets will only have an 8 digit obsID and will have negative exposure_a and exposure_b values. The planned targets include approved targets from the *XMM-Newton* AO13, *Suzaku* AO9 and *Chandra* AO16 joint programs as well as targets in the *NuSTAR* legacy surveys.
RPS input: Investigations involving sources previously observed or currently planned for observation with *NuSTAR* must provide a justification of the need for the requested additional data. A list of planned *NuSTAR* observations is also available on the *NuSTAR* homepage (http://nustar.caltech.edu).

Additional response files for use with XSPEC
• Useful for generating ARF for evaluation using "fakeit" command within XSPEC • Standard response files are for point sources on-axis • Additional response files are available for evaluation of off-axis and extended sources
URL: http://www.nustar.caltech.edu/page/response_files
Notes: See section 4.4 for details about *NuSTAR* response files
RPS input: Proposers should provide an evaluation of the feasibility of observations of sources expected to be non-point like and/or located away from the optical axis on the *NuSTAR* detectors.

4.4 *NuSTAR* Response Files

All response files represent the response of **one** *NuSTAR* telescope. The two *NuSTAR* telescopes (labeled by their focal plane modules, FPMA and FPMB) have subtly different responses and explicitly combining data from FPMA and FPMB when performing data analysis is not recommended (i.e., combining individual counts from both telescopes to make a single spectrum). Science users should simulate the source spectrum twice and use simultaneous fitting when determining the feasibility of an observation.

A *NuSTAR* response file (nustar.rmf) is constructed from real data for sources near the optical axis of either telescope and varies relatively little between FPMA and FPMB. Background files should be paired with a similar source extraction region (e.g., use the 30-arcescond background region for the 30-arcsecond source extraction region ARF, not with the 60-arcsecond extraction region ARF). To facilitate more accurate simulations, a set of response files are available to be used with XSPEC "fakeit" - or another observatory simulator. We divide the sources into point-like sources and extended sources.

- Point Sources

  If the proposed target is a point source, the only distinction to be made is whether or not it qualifies as strong or weak. For stronger sources a 60-arcsecond radius circular extraction region is recommended, while for a weaker sources a 30-arcsecond radius circular extraction region should be used. For *NuSTAR* data analysis the source extraction size can be varied to determine the optimal signal-to-noise. For simulating sources, it may not be apparent whether a source is "strong" or "weak", so simulating source extraction using both 30" and 60" extraction regions can be performed to determine an optimal signal-to-noise for a particular exposure time.

Standard observations of point sources usually place the target between 1 and 3 arcminutes away from the optical axis of the telescope, refer to the distance between the optical axis and the source as the "off-axis angle" (see section 9.3). Response files that span the likely off-axis angle distance at 1, 3 and 5 arcminutes are available in a tar archive file from the *NuSTAR* website at

> http://www.nustar.caltech.edu/page/response_files

If there is just one source in the FOV to be evaluated, then the 1arcminOA response files and background should be used. See the section 4.7.1 for examples of simulating a point source within XSPEC.

- Extended Sources

  If the proposed target is an extended source, then the amount of area over which the photons are distributed on the sky needs to be specified. We have used the PWNe G21.5+0.9 and the SNRs Cas A and Tycho to generate representative response files for objects with a projected radius on the sky of 1, 3, and 5 arcminutes. All three sources are roughly spherical and have roughly constant surface brightness. Note that if a source is composed of "knots" superposed on an extended target, then a proposer should separately simulating the knots using the ***point source*** response files.

See section 4.7.2 for examples of simulating an extended source within XSPEC.

4.5 Simulating *NuSTAR* Countrate with WebPIMMS

The online tool WebPIMMS can be used to quickly estimate the expected countrate for a source to be observed by *NuSTAR*. WebPIMMS is available on the HEASARC website at:

> http://heasarc.gsfc.nasa.gov/cgi-bin/Tools/w3pimms/w3pimms.pl

NUSTAR

PIMMS predicts 1.179E-02 cps with NUSTAR
(For both modules for a 50% PSF extraction without accounting for deadtime)

```
 * Count rates in different energy bands
 * The dead time value  assumed is 0.0025 sec
 * The dead time fraction is estimated to be  0.0%

   band      counts/s     counts/s   counts/s
            ---------    both modules  --------

   (keV)     no dead time background with dead time
   3-79      1.179E-02    4.715E-03  1.17929E-02
   3-10      8.798E-03    1.393E-03  8.79761E-03
   10-20     2.372E-03    5.960E-04  2.37223E-03
   20-40     5.309E-04    1.430E-03  5.30889E-04
   40-79     9.201E-05    1.296E-03  9.20038E-05

 The source is detectable at  5 sigma in  2.96749E+03  seconds (3-79 keV)
 The source is detectable at  3 sigma in  1.06830E+03  seconds (3-79 keV)
```

This tool allows users to convert from flux or observed count rates from historical and operating missions (e.g. *ASCA, ROSAT, Chandra*-ACIS, *XMM*-MOS, etc) into *NuSTAR* count rates. Set the "Into:" option to "NuSTAR" and use the default output energy range. Simple source models are available in the basic tool and more complicated models can be simulated through the multiple model component interface. The box to the left is an example of the output from WebPIMMS for an absorbed powerlaw model ($\Gamma = 1.9$, $N_H = 10^{20}$ cm^{-2}) based on a *ROSAT*-PSPC count rate of 0.1 counts/s.

An estimate of the *NuSTAR* count rate is required for all observations in the GO RPS target proposal form in the "Expected Count Rate Above Background" field. If WebPIMMS is used to estimate *NuSTAR* count rates then the value for the 3-79 keV count rate with no dead time should be quoted on the RPS form, e.g. 0.012 from the above example (highlighted). This count rate is for both *NuSTAR* modules using a 50% PSF extraction region with no dead time correction.

4.6 Simulating *NuSTAR* Data Using WebSpec

WebSpec provides an online facility for simulating spectra for a variety of combinations of missions and instrument using several different physical models and is available through the HEASARC website at:

http://heasarc.gsfc.nasa.gov/webspec/webspec.html

It utilizes XSPEC and thus has similar inputs and produces similar results to an XSPEC fit (see section 4.7). There are currently two ways to run WebSpec. First, there is the initial WebSpec page, which provides a straightforward means for specifying the desired model. The more experienced XSPEC user may wish to use the more advanced WebSpec interface:

http://heasarc.gsfc.nasa.gov/webspec/webspec_advanced.html

Below is an example output from the standard WebSpec simulation of a *NuSTAR* observation of a source with an absorbed powerlaw model ($\Gamma = 1.9$, $N_H = 1 \times 10^{20}$ cm^{-2}) and a 50 ksec exposure.

This is a (Photoelectric Absorption)((Power Law)) simulation of a NUSTAR.50PCT observation of 50000 seconds. The actual model expression used by xspec was zphabs*zpowerlw .

This model resulted in a C-statistic of 1099.66 and a count rate of 0.012095 cts/s over the fitted energy range.

The best fit parameters and errors for this simulated data set are:

For the Photoelectric Absorption component:

Hydrogen Column	1.36855	+ 2.267 - 1.369	10^22 atoms/cm^2
Redshift	0		

For the Power Law component:

Photon Index	1.86748	+ 0.044 - 0.043
Redshift	0	
Normalization	0.00013	

Resulting fluxes:

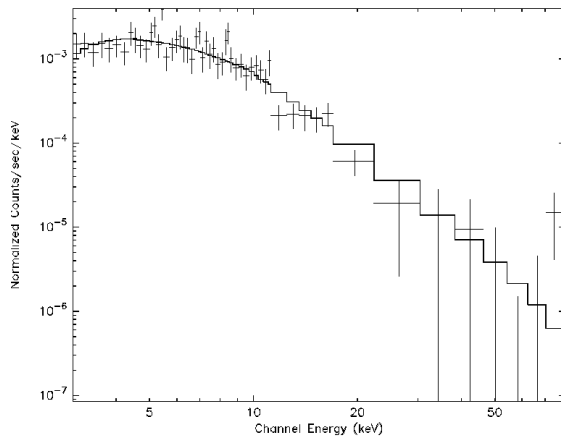| Energy Band	Low Energy	High Energy	Count Rate (counts/sec)	Photon Flux (ph/cm^2/s)	Energy Flux (ergs/cm^2/s)
1	3.0	80.0	0.012095	5.15511e-05	9.70727e-13

Figure 14 WebSpec simulated spectrum for absorbed powerlaw model ($\Gamma = 1.9$, $N_H = 1$ x 10^{20} cm^{-2}) and a 50 ksec exposure.

4.7 Simulating *NuSTAR* Data using XSPEC

NuSTAR data can be simulated within the XSPEC[15] package by utilizing the fakeit command and using the response files available from the *NuSTAR* webpage (see section 4.4). The XSPEC software package is freely available from the HEASARC website:

http://heasarc.gsfc.nasa.gov/xanadu/xspec/

In the examples below it is assumed that the user has installed the XSPEC package (in this case v12.8.1 is used) and downloaded the *NuSTAR* response files.

4.7.1 Simulated point source close to the optical axis

Optimal *NuSTAR* observations will place the source within 1 arcmin of the telescope optical axis location on the detectors (see section 8.3 for details).

These following XSPEC thread shows the minimal steps required to simulate a simple powerlaw model ($\Gamma= 1.9$) spectrum. The responses from XSPEC to the commands are highlighted in grey.

First, set up the model for the simulated spectrum:

XSPEC12> model powerlaw

```
Input parameter value, delta, min, bot, top, and max values for ...
        1    0.01(   0.01)    -3    -2    9    10
1:powerlaw:PhoIndex>1.9
        1    0.01(   0.01)     0     0   1e+20   1e+24
2:powerlaw:norm>1
```

```
========================================================================
Model powerlaw<1> Source No.: 1   Active/Off
Model Model Component  Parameter  Unit    Value
 par  comp
   1   1   powerlaw   PhoIndex            1.90000    +/-  0.0
   2   1   powerlaw   norm                1.00000    +/-  0.0
```

XSPEC12> flux 2 10

```
Model Flux   0.78231 photons (5.6119e-09 ergs/cm^2/s) range (2.0000 - 10.000 keV)
```

Adjust the model normalization to set the flux to the desired level. E.g. for a 2-10 keV flux of 1 x 10^{-11} erg cm^{-2} s^{-1}

XSPEC12> newpar 2 3.33e-3

XSPEC12> flux 2 10

> Model Flux   0.001519 photons (1.0012e-11 ergs/cm^2/s) range (2.0000 - 10.000 keV)

Generate the simulated data (fake_source_1) for a 150 ksec exposure using the background data for a 30 arcsec extraction region (bkgd_30arcsec.pha), with the *NuSTAR* response file (nustar.rmf) and a point source at 1 arcmin from the optical axis (point_30arcsecRad_1arcminOA.arf):

XSPEC12> fakeit bgd_30arcsec.pha

> For fake spectrum #1 response file is needed: nustar.rmf
> ...and ancillary file: point_30arcsecRad_1arcminOA.arf
> Use counting statistics in creating fake data? (y): y
> Input optional fake file prefix: fake_source_1
> Fake data file name (fake_source_1nustar.fak): fake_source_1.fak
> Exposure time, correction norm, bkg exposure time (244003., 1.00000, 244003.): 150e3

> 1 spectrum in use
>
> Fit statistic : Chi-Squared =   1962.17 using 4096 PHA bins.
>
> ***Warning: Chi-square may not be valid due to bins with zero variance
>   in spectrum number(s): 1
>
> Test statistic : Chi-Squared =   1962.17 using 4096 PHA bins.
> Reduced chi-squared =   0.479278 for   4094 degrees of freedom
> Null hypothesis probability =   1.000000e+00
>
> ***Warning: Chi-square may not be valid due to bins with zero variance
>   in spectrum number(s): 1
>
> Current data and model not fit yet.

To estimate the error range for the model parameters for this simulated 150 ksec exposure we should use C statistics and set the energy range to the *NuSTAR* band (3 – 78 keV):

XSPEC12> statistic cstat

XSPEC12> ignore **-3.0 78.0-**

Now try a fit of the model to the simulated data:

XSPEC12> fit 100

> ```
>                    Parameters
> C-Statistic  |beta|/N   Lvl   1:PhoIndex     2:norm
> 1523.53     19590.3     -3      1.92566    0.00347788
> 1523.51     2773.87     -4      1.92557    0.00348074
> 1523.51     7.36181     -5      1.92557    0.00348071
> ============================
>  Variances and Principal Axes
>             1      2
>  1.9696E-04| -1.0000  -0.0069
>  6.2343E-10|  0.0069  -1.0000
>  ----------------------------
> ```

```
                    Parameters
C-Statistic  |beta|/N   Lvl   1:PhoIndex      2:norm
1523.53     19590.3    -3     1.92566    0.00347788
1523.51     2773.87    -4     1.92557    0.00348074
1523.51     7.36181    -5     1.92557    0.00348071
==============================
 Variances and Principal Axes
           1        2
 1.9696E-04| -1.0000  -0.0069
 6.2343E-10|  0.0069  -1.0000
------------------------------


=======================
 Covariance Matrix
      1        2
  1.970e-04   1.365e-06
  1.365e-06   1.008e-08
-----------------------
======================================================================
Model powerlaw<1> Source No.: 1   Active/On
Model Model Component  Parameter  Unit     Value
 par comp
   1   1   powerlaw   PhoIndex           1.92557      +/-  1.40340E-02
   2   1   powerlaw   norm               3.48071E-03  +/- 1.00424E-04
```

The 90% confidence range for the model parameter(s) can be found using the error command

    XSPEC12> error

```
Parameter   Confidence Range (2.706)
    1     1.90286     1.94835    (-0.0227064,0.0227861)
```

Which appears to not be close to the model for the simulated data ($\Gamma = 1.9$). However the simulated background could be affecting the fitting. The simulated data and background spectrum should be plotted to investigate the relative level of source and background flux.

Set the plot window to use units of keV and to rebin the data channels to 20 σ significance (or groups of 20 channels):

    XSPEC12> cpd /xs

    XSPEC12> setplot energy

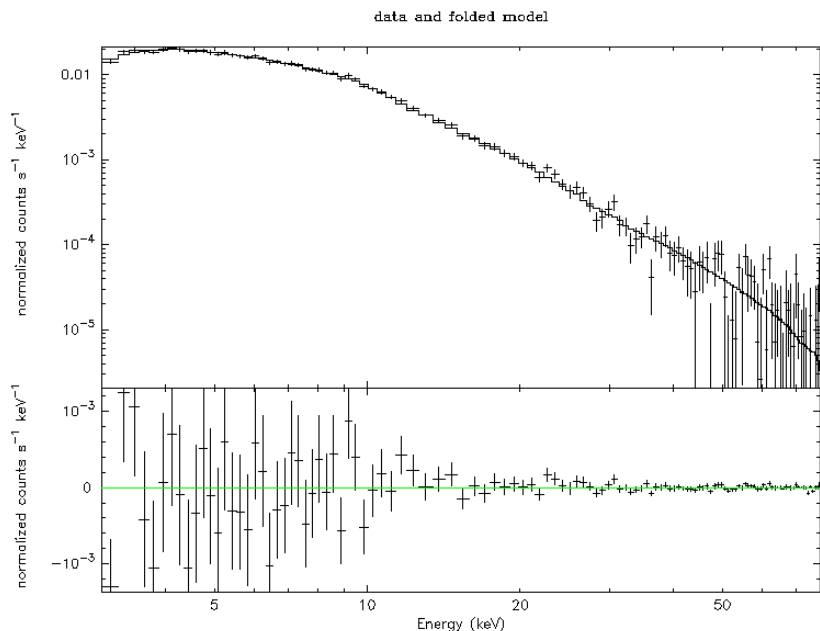   XSPEC12> setplot rebin 20 20

    XSPEC12> plot ldata res

Figure 15 XSPEC plot of a simulated powerlaw spectrum. Top – Simulated data and model. Lower – Residuals from data to model fit.

Investigate the background spectrum:

> XSPEC12> setplot back

> XSPEC12> plot

data and folded model

Figure 16 XSPEC plot of simulated powerlaw spectrum. Spectrum of simulated background is shown as thick points.
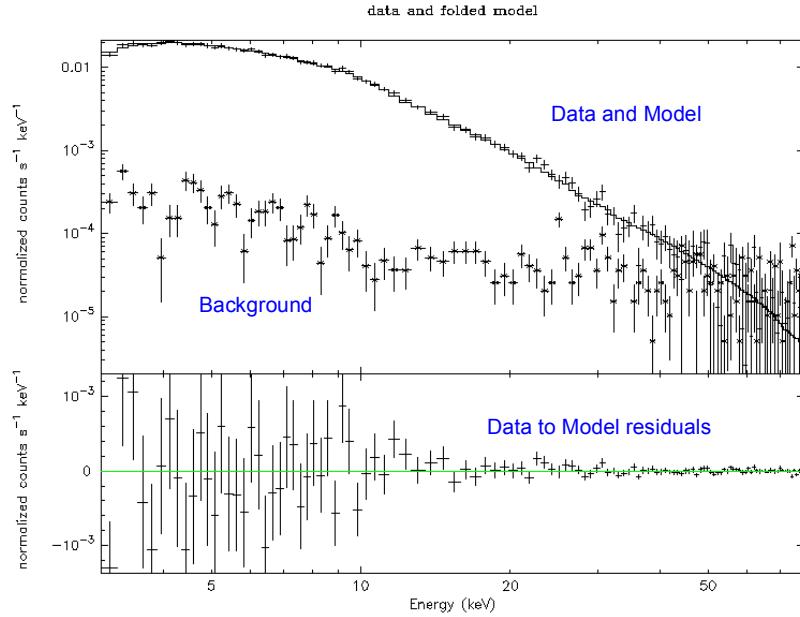
The background flux becomes significant at around 50 keV. So the model fitting can be limited to < 50 keV using the ignore commend:

> XSPEC12> ignore 50.0-**

> XSPEC12> fit

```
                    Parameters
C-Statistic |beta|/N  Lvl  1:PhoIndex     2:norm
1168.27     5178.8    -3     1.91098   0.00338618
1168.27     1175.36   -4     1.91060   0.00338499
==============================
 Variances and Principal Axes
           1        2
 1.9555E-04| -1.0000  -0.0067
 5.8952E-10|  0.0067  -1.0000
----------------------------


========================
  Covariance Matrix
     1        2
  1.955e-04   1.320e-06
  1.320e-06   9.494e-09
-----------------------


=====================================================================
Model powerlaw<1> Source No.: 1   Active/On
Model Model Component Parameter Unit    Value
 par comp
  1   1   powerlaw  PhoIndex        1.91060     +/-  1.39838E-02
  2   1   powerlaw  norm            3.38499E-03 +/-  9.74376E-05
_____


Fit statistic : C-Statistic =       1168.27 using 1174 PHA bins and 1172 degrees of freedom.

Test statistic : Chi-Squared =       1328.08 using 1174 PHA bins.
 Reduced chi-squared =       1.13317 for   1172 degrees of freedom
 Null hypothesis probability =   9.532521e-04
```
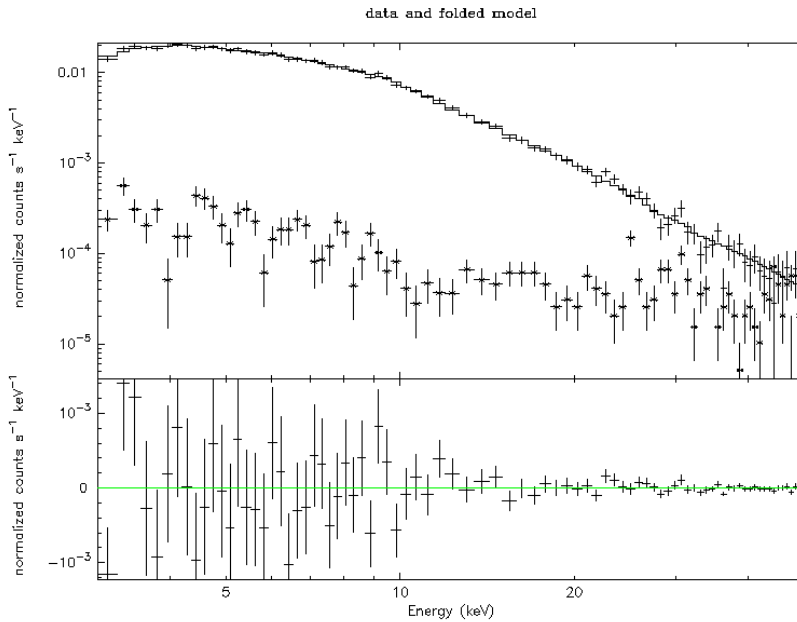
23

data and folded model

Figure 17 XSPEC plot of simulated powerlaw spectrum and background, restricted to < 50 keV.

XSPEC12> error

Parameter   Confidence Range (2.706)
    1   1.88766   1.93361   (-0.0229331,0.0230158)

Which is consistent with the input powerlaw model slope. XSPEC simulations using *NuSTAR* response files are for **one** telescope only.

More complex models can be simulated with XSPEC and proposers can investigate the effects of using a larger extraction region (60 arcsec radius) and positions further from the optical axis (3 & 5 arcmin) using the available response files.

Table 7 *NuSTAR* response files for simulating point sources.

point_30arcsecRad_1arcminOA.arf point_30arcsecRad_3arcminOA.arf point_30arcsecRad_5arcminOA.arf	"Point" source ARF's extracted using a circular extraction region with a radius of 30 arcseconds. Off-axis angle 1, 3, 5 arcminutes
point_60arcsecRad_1arcminOA.arf point_60arcsecRad_3arcminOA.arf point_60arcsecRad_5arcminOA.arf	"Point" source ARF's extracted using a circular extraction region with a radius of 60 arcseconds. Off-axis angle 1, 3, 5 arcminutes
bgd_30arcsec.pha bgd_60arcsec.pha	Background for 30 and 60 arcsecond radius extraction regions
nustar.rmf	Response file for sources near the optical axis.

24

4.7.2 Extended source simulation

Simulating the spectrum from an extended source can follow the same methodology for point sources outlined in the previous section. The pairs of background PHA and source extraction ARF files are given in table 8 below. Note that the response files are for ONE of the two *NuSTAR* telescopes. The RMF and ARF files were generated using the NuSTARDAS module *nuproducts* with the "extended" source option, while the background PHA file was simulated using the NUSKYBKGD simulation toolkit (Wik et al., 2014)[13].

Table 8 *NuSTAR* response files for simulating data from extended sources.

Approximate radius of source		ARF / PHA file pair
1 arcminute	These set of response and background files were generated using a ~134 ksec observation of G21.5-0.9. The ARF was generated using the "extended" source option in NuSTARDAS for the 1 arcminute radius circle centered on the source with the optical axis roughly centered on the SNR.	extended_1arcminRad.arf bgd_1arcmin.pha
3 arcminutes	These set of response and background files were generated using a ~294 ksec observation of Cassiopeia A. The ARF was generated using the "extended" source option for the 3 arcminute radius circle centered on Cas A with the optical axis roughly centered on the SNR.	extended_3arcminRad.arf bgd_3arcmin.pha
5 arcminutes	These set of response and background files were generated using a ~340 ksec observation of Tycho. The ARF was generated using the "extended" source option for the 5 arcminute radius circle centered on Cas A with the optical axis roughly centered on the SNR.	extended_5arcminRad.arf bgd_5arcmin.pha

5. DATA ANALYSIS

NuSTAR data analysis is performed using a software package called **NuSTARDAS** developed at the ASI Science Data Center (ASDC, Italy) in collaboration with the *NuSTAR* SOC. The design of the NuSTARDAS pipeline software and calibration files is based on community standard implementations used in analysis of data from high energy astrophysics observatories. This reduces the data analysis effort because of the community's familiarity with standard tools and protocols. NuSTARDAS is fully compatible and integrated with the **HEASoft** software package, maintained and distributed by the NASA-HEASARC data center, and is officially distributed to users within its standard public software releases.

The NuSTARDAS package produces cleaned and calibrated detector event list files and standard high-level scientific products, starting from the FITS formatted telemetry data following the NASA-OGIP standards[16]. The software is designed as a collection of modules (tasks), written in the HEASoft FTOOLS style, each dedicated to a single function. The package also includes a pipeline processing script (*'nupipeline'*) allowing users to automatically run in sequence all the tasks required for data processing.

The *NuSTAR* software parameter interface is implemented with the HEASoft Parameter Interface Library and the I/O with the FITS data files makes use of the FITSIO library[17]. NuSTARDAS makes exclusive use of open source software (C and Perl languages) and multi-mission FTOOLS from the HEASoft package are also used in several NuSTARDAS modules. NuSTARDAS tasks retrieve observatory calibration files that are complaint with the standard structures of HEASARC's calibration database (CALDB) system.

5.1 Data Processing Stages

The input to the NuSTARDAS package is the level-1 (L1) *NuSTAR* FITS formatted telemetry data produced at the SOC from L0 raw telemetry files. NuSTARDAS data processing is organized in three distinct stages for the calibration, screening, and the extraction of high-level scientific products as illustrated in Figure 18 which lists the FTOOLS packages used at each stage of processing.
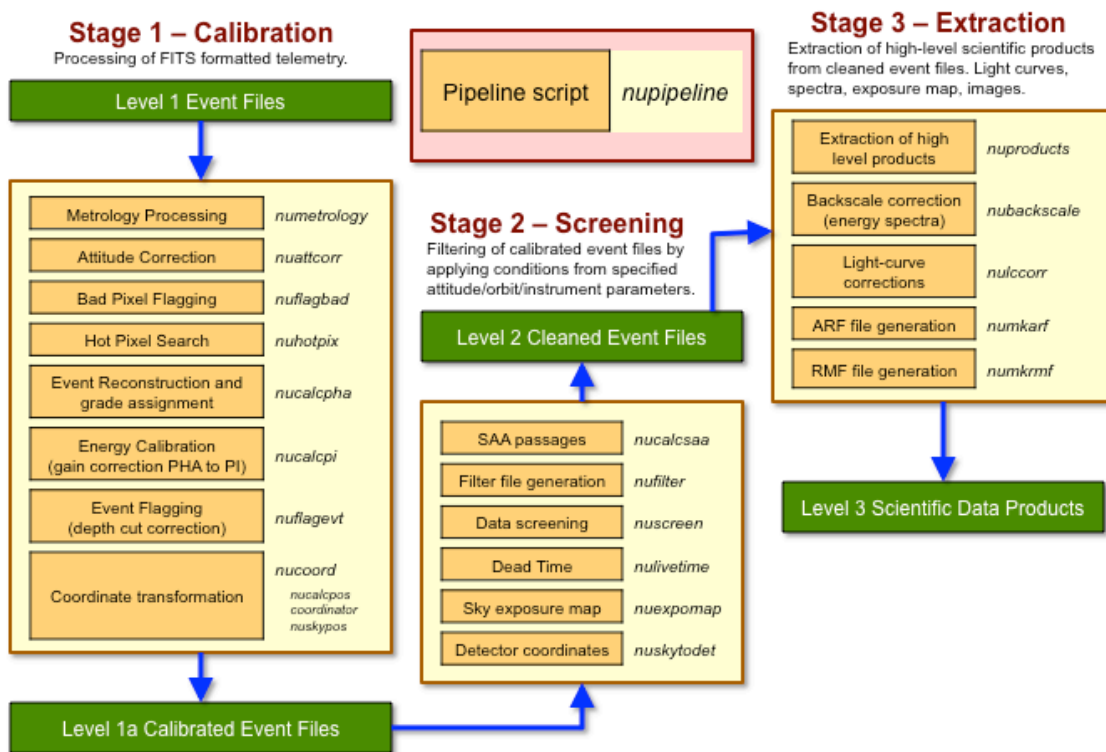

Figure 18 NuSTARDAS data processing stages. The *nupipeline* script controls the order of execution of the processing tasks and contains the parameters associated with each stage of processing.

These three main processing stages are:

1. **Data Calibration**: FITS formatted telemetry processing to produce calibrated event files (L1a);

2. **Data Screening**: Calibrated event files are filtered by applying cleaning criteria on specified orbital/instrument parameters and event properties to produce cleaned event files (L2);

3. **Products Extraction**: High-level scientific products are generated (light-curves, energy spectra, sky images, Ancillary Response Files, Redistribution Matrix Files) (L3);

The files generated with the NuSTARDAS package (e.g. Level 1a/2 event files, Level 3 energy spectra and light-curves) can be read into HEASoft data analysis programs such as XSELECT, XSPEC, XRONOS and XIMAGE[18].

The NuSTARDAS package is automatically run at the SOC using standard parameters when new L0 files become available after each ground station pass, so that each observation can be monitored as exposure time is built up to completion.

Figure 18 below shows an example of *NuSTAR* data processing for the 11 orbit observation of Swift J1753.5-0127 on 2014-04-04 (ObsID 80002021002). The top plot shows the time variation of raw detector countrate on one detector (DET0 in FPMA). The drop of total countrate can clearly be seen as the target is occulted by the Earth each orbit during the observation (marked 'O' in middle panel). An increase in background events can also be seen during each SAA passage (marked 's' and 'S' in the middle panel). The drop to zero countrate in the middle of some SAA passages starts when the detector shield event rate reaches the SAA passage threshold. This stops the recording of X-ray events from the CZT detectors, until the shield event rate drops below the threshold level upon exiting from the SAA.
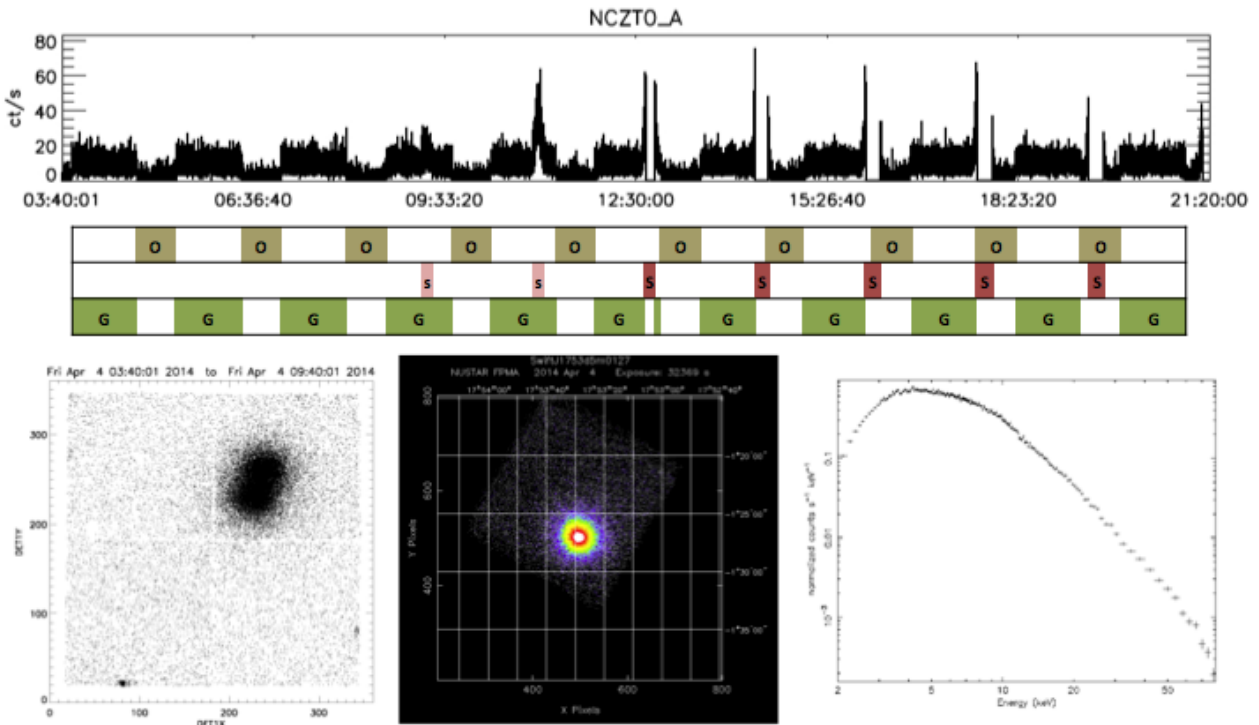
Figure 19 *NuSTAR* data processing example (ObsID 80002021002). *Top* - Raw L0 event rates measured by one of the four CZT detectors (DET0) on FPMA. *Middle* - Example screening of the data. Good time intervals (G) are determined by screening out periods of Earth occultation (O) and SAA passage (S). *Lower* – (*Left*) L1 image from FPMA in detector coordinates. High level data products from stage 3 data processing include images of the observation in sky coordinates (*middle*) and calibrated energy spectra of events extracted around the location of the science target (*right*).

The middle panel of Figure 19 illustrates the standard screening of data from the detectors during the observation. Good Time Intervals (GTI, G) for science analysis are determined by screening out periods of Earth occultation (O) and SAA passage (S). Orbits where the shield event rate does not rise to the SAA passage threshold level (s, light red) are not screened out with standard processing parameters. A more stringent screening based on higher background X-ray countrate periods can be performed using specific parameters within *nupipeline* (see section 8.1 below).

The last three plots in Figure 19 show an image of FPMA in detector coordinates for the observation. Note that the target is located in the nominal position on DET0 with events from the astrophysical source spread out due to aspect motion during the observation (see section 8.3 below). Aspect reconstruction of the events to the sky plane is performed in stage 1 of NuSTARDAS processing. Note also the small gaps between the four CZT detectors on the focal plane and the presence of 'hot' pixels on the edges of the detectors that are flagged in stage 1 and screened out in phase 2 of data processing. High level data products from stage 3 of NuSTARDAS processing include images of the observation in sky coordinates (*middle*) and calibrated energy spectra of events extracted around the location of the science target (*right*).

5.2 Public Access to NuSTARDAS

The NuSTARDAS package has been designed to allow the community to reproduce any stage of the *NuSTAR* data processing, which could be necessary, for example, because of improved calibration information, or updated software modules. It is also often the case that detailed scientific analysis of observations requires use non-standard data processing settings and this is achieved through the interface of parameters in the *'nupipeline'* script and the NuSTARDAS packages.

NuSTARDAS is integrated within the HEASoft X-ray data analysis package and can be freely downloaded from HEASARC:

http://heasarc.gsfc.nasa.gov/docs/software/lheasoft/

and is available for multiple operating system platforms. A software users guide with detailed information and processing examples is available on the *NuSTAR* archive website:

http://heasarc.gsfc.nasa.gov/docs/nustar/index.html

Updates to NuSTARDAS are expected throughout the mission as refinements of data processing tools become available.

6. DATA ARCHIVE

The adoption of common standards for data formats, calibration and analysis software by the high energy astrophysics community started in 1990 with the creation of the NASA's High Energy Astrophysics Science Archive Research Center (HEASARC) at the Goddard Space Flight Center in Greenbelt, MD. HEASARC pioneered a model of data centers staffed by research scientists that has been adopted by science archives for infrared (IRSA, Caltech[19]) and optical/UV (MAST, STSci[20]) astronomical data. The data and software standards developed by the HEASARC provide the underlying infrastructure for the curation and interpretation of data from a wide variety of missions, substantially reducing mission costs while increasing science return.

HEASARC is the primary archive for *NuSTAR* data, calibration files and data analysis software. The HEASARC's archive services allow scientists to identify, display, cross-correlate, download and analyze data from a variety of past and active missions – including *ASCA, BeppoSAX, Chandra, CGRO, Einstein, Fermi, INTEGRAL, ROSAT, RXTE, Suzaku, Swift, WMAP* and XMM-Newton – and provides access to a wide range of multiwavelength sky surveys, astronomical catalogs and other resources.

The *NuSTAR* data archive is also mirrored at the ASI Science Data Center (ASDC, Rome) that supports a multi-mission archive for European space astrophysics.

6.1 numaster Catalog

NuSTAR data is organized into periods of time associated with ObsID's, with no gaps during the mission, tabulated in a master catalog (*numaster*). This catalog is generated by the SOC and consists of a list of ObsID's that have been processed and validated by the SOC. The structure of the data archive is governed by information in the numaster catalog, including the public release dates of each ObsID. The community can search for data of interest using the standard HEASARC tools BROWSE and XAMIN that contain the metadata from the numaster catalog.

6.2 Data Transfer and Release Schedule

NuSTAR data is transferred to the archives using a PERL script for SFTP data transfer originally developed for the *XMM-Newton* satellite and upgraded for multi-mission use (DTS[21]). The DTS performs multi-directional transfer from one site to several others, compress and decompress files on-the-fly, splits and recombine files, reconstitute directory structures, clean up staging areas, and activate external scripts, all automatically or on the command line.

All *NuSTAR* data will eventually become publically available at the archives after a 60 day validation period at the SOC commencing after the end of an observation. Exceptions are made for observations taken as part of joint programs with other observatories, and for data taken as part of the *NuSTAR* guest observer program, where a one year limited use period is provided to the proposer. *NuSTAR*'s first public release was in August 2013 and subsequent releases have been ~two months apart.

7. OBSERVATION PLANNING

NuSTAR was designed to be able to access 80% of the sky at any time and to stare at a location on the celestial sphere for periods as long as a month with a duty cycle of > 50%. This observatory efficiency is primarily determined by the occultation of a target by the Earth during each orbit. The detectors remain active during slew and Earth occultation, essentially recording instrumental background. Each observation thus consists of an occulted and un-occulted period each orbit with exposure time built up over multiple orbits in ~3200 second exposures. The duration of each un-occulted period depends on the celestial coordinate of the target and plane of the *NuSTAR* orbit at the time of the observation. The *NuSTAR* orbit inclination is 6° so for targets with low Declinations (|Dec| < 55°) there is at most a 15% range in un-occulted duration over the ~50-day nodal precession period. Targets at higher Declinations have a larger variation of available exposure time and for observations with exposure time goals that will take longer then one day to achieve, these higher efficiency dates are taken into account during target scheduling.

Other considerations for scheduling observations include:

- Passage of the spacecraft through the **South Atlantic Anomaly** (SAA) where the higher level of particle induced background is detected by the anti-coincidence shielding. During these passages the CZT detectors remain active but the X-ray events are not recorded because the increased background would swamp the signal from astrophysical sources (and increase onboard data accumulation). SAA passages occur in approximately 50% of all orbits and can last between 120s and 850s as the *NuSTAR* orbit latitude precesses through the SAA. Although the maximum impact of SAA passage can reduce the available exposure time in one orbit by 25%, most *NuSTAR* observations are longer the 7 orbits and the SAA passage time will move into the target Earth occultation period during the observation. So on average the impact of SAA passage on the available exposure time for any observation is < 10%.

- The *NuSTAR* X-ray telescopes are designed to enable Solar observations but for all other targets the **Sun avoidance angle** is determined from the constraints on the absolute pointing determination from the star tracker mounted on the optics bench (called CHU4). The baffling around CHU4 enables valid attitude solutions when the Sun is > 39° from the telescope boresight. However, it was determined before launch that for Sun angles between 40° and 50° there could be an uncertainty in orientation of the spacecraft solar array assembly in the event of a spacecraft anomaly. So the operational limit for Sun avoidance is set to > 50°.

- **Moon avoidance** is determined from measurements of CHU4 performance during observations close to the full Moon and is set to > 14°. Observations can be performed below this limit at lower illumination phases of the Moon but the impact on scheduling due to this constraint is at most one day per month and no observations in the first two years of science operations have been performed below this constraint.

- *NuSTAR* spacecraft attitude is determined from three star tracker cameras mounted on the spacecraft bus (called CHU1,2,3). One of these cameras must provide a valid attitude solution at all times and there are some spacecraft orientations where all three cameras are blocked by a combination of the Sun, Earth, or Moon. This **CHU blockage** constraint can result in periods of up to 3 days where an observation of a particular target cannot be scheduled.

- **Position angle.** The *NuSTAR* field of view is square and the optimal location of a target on the focal plane is not in the center of the field of view but located as close as possible to the optical axis of the telescope, where effective area is highest. Some observations, particularly of extended sources or survey observations with overlapping tiles, have constraints on the position angle during an observation. A position angle requirement for an observation results in a scheduling constraint because the power and thermal limit constraints for the spacecraft determine the angle of the telescope boresight to Sun-Earth vector. There is a 10 degree margin allowed for this constraint and the consequence is that a particular position angle can only be maintained for a limited duration, from 5 days to a few months depending on the ecliptic latitude of a target (see Figure 20).
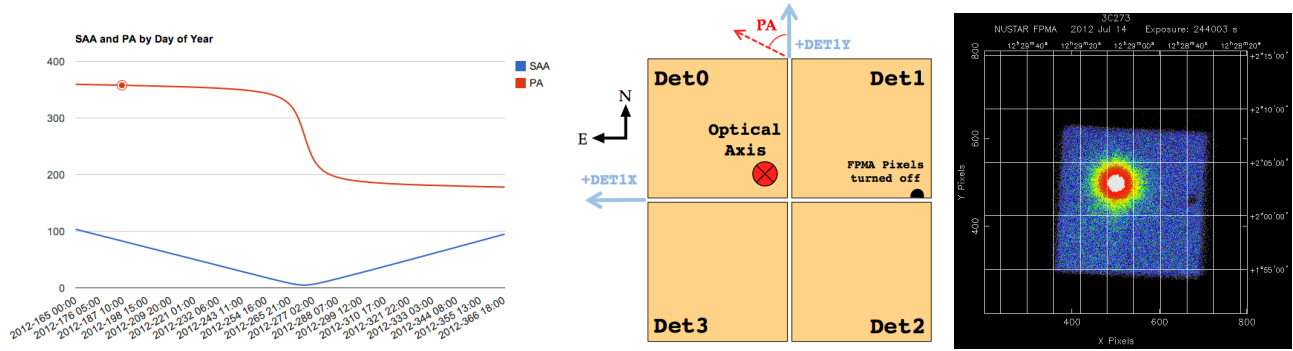
Figure 20 *Left* - Example of the variation of position angle (PA) and solar aspect angle (SAA) for 3C 273 (J2000 187°.278 +2°.052) during June-Dec 2012. *Center* - Definition of position angle of *NuSTAR* field of view and nominal location of the optical axis approximately 3mm (60″) from the center of the field of view, located on DET0. *Right* - Image from the observation of 3C273 on 2012-07-14 at PA = 355° (ObsID=10002020001).

An example of the variation in observation efficiency is shown in Figure 21 below for 3C 273 (J2000 187°.28 +2°.75) and NGC 3516 (J2000 166°.70 +72°.57). Periods with a Sun avoidance constraint are marked in red, the Moon and CHU blockage constraints are indicated in blue and green respectively. The available exposure time each day is calculated based on the most recent *NuSTAR* orbital ephemeris. The day with the most recent TLE measurement is marked with a blue dashed line (2014:119). Exposure times after that date are predictions based on that TLE. The middle and lower plots show an expansion of the daily exposure time trend close to day of most recent TLE. The overall modulation is due to changes in the duration of Earth occultation for the targets over the 50-day nodal regression period with a daily variation superimposed over that trend due to SAA passage events that occur in the un-occulted periods. Note that the high Declination of NGC 3516 provides periods of continuous viewing (e.g. DOY 122 – 132), modulated only by SAA passages (-3 ksec per day) and CHU blockage constraints.
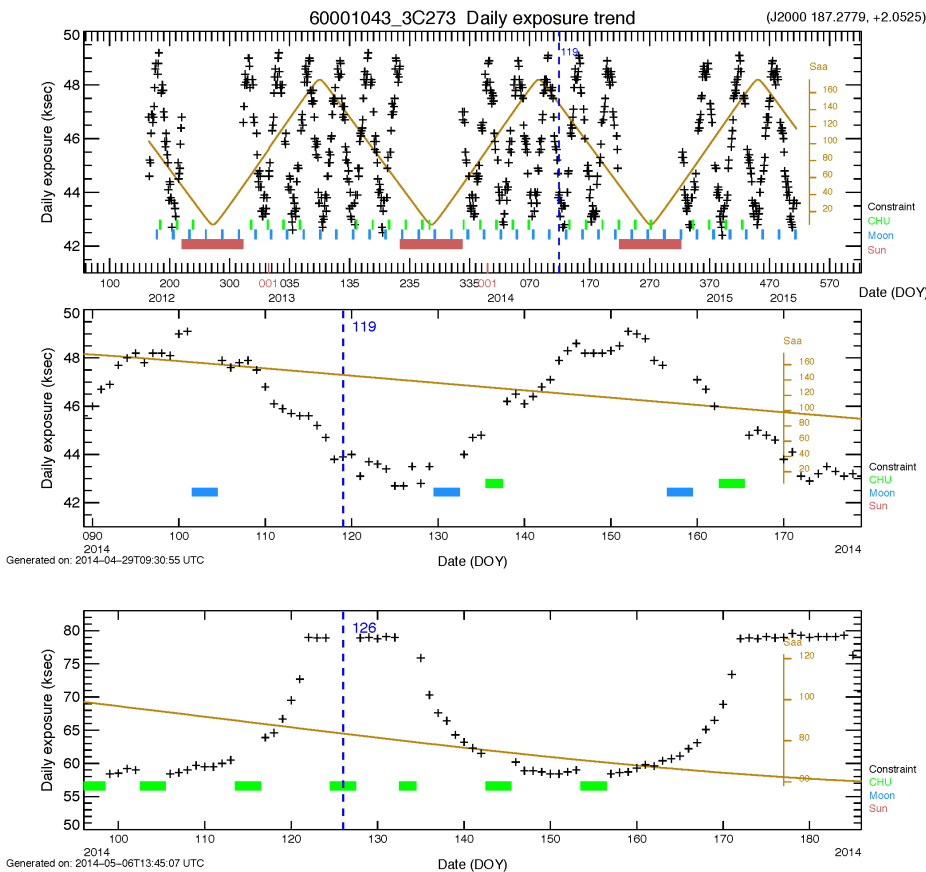

Figure 21 Observation efficiency plots for two targets of different Declinations. *Top* - Modulation of available exposure time each day for 3C 273 (Dec +2°.05) from June 2012 to May 2015. The average Solar aspect angle (Saa) each day is also plotted (yellow). *Lower* - Available exposure time trend for NGC 3516 (Dec +72°.57).

31

Note that the decay of the *NuSTAR* orbit can be unpredictable depending on Solar activity and variations in atmospheric drag, so it is possible for inaccuracies in predictions based on a particular TLE to propagate through the efficiency predictions and indicate unusual changes in observation efficiency. So the optimal time for an observation to be scheduled is within 5 days of predicted peak efficiency.

7.1 Coordinated Observations

NuSTAR complements observations using current soft X-ray observatories like *Chandra*, *XMM-Newton, Suzaku*, and *Swift* and is a bridge to low resolution coded mask instruments operated in the hard X-ray band by *INTEGRAL, Fermi,* MAXI, and *Swift*-BAT. The utility of simultaneous soft and hard X-ray observations has resulted in a collaboration between the *NuSTAR* and *Swift* missions. Almost all *NuSTAR* observations since launch have simultaneous *Swift*-XRT observations of 2 ksec or more with the XRT data publically available. Joint observation programs have also been offered to the community within the proposal calls for *XMM-Newton* and *Chandra* observatories with *NuSTAR* observing time allocated before the implementation of a *NuSTAR* guest observer program.

The level of coordination with other observatories, including ground-based observatories like HESS, MAGIC, and VERITAS, is unprecedented for a new mission; with more then 15% of all *NuSTAR* observations requiring some coordination of scheduling. Scheduling constraints for *NuSTAR* are mild in comparison with other space observatories and so the *NuSTAR* schedule will most often follow the timing of observations for other observatories.

Table 9 Coordinated *NuSTAR* observations during the two-year primary mission (up to 2014-06-20).

Observatory	# Coordinated targets	# Coordinated exposures
XMM-Newton	29	48
Chandra	11	16
Suzaku	15	20
INTEGRAL	7	10
HESS, MAGIC, VERITAS	3	30
Swift	*Nearly every NuSTAR target (>400)*	
HST & Spitzer	4	6

7.2 ToO and DDT

NuSTAR is designed to be able to access 80% of the sky at any given time and this makes it a powerful telescope for Target of Opportunity (ToO) investigations. The importance of 'unplanned' observations has been recognized by the project and 15% of the time in the *NuSTAR* extended mission has been allocated to ToO observations solicited as part of directors' discretionary time (DDT). This will allow a better assessment of the feasibility of each observation on a case-by-case basis. ToO and DDT requests can be submitted from the *NuSTAR* website at:

http://www.nustar.caltech.edu/page/too_policy

A justification for the requested observation(s) must be included, including justification for fast ToO responses.

8. OBSERVATORY ON-ORBIT PERFORMANCE

The observatory is performing on-orbit within expectations but, as with any new instrument, some adjustments have been required to respond to observatory characteristics that were not fully understood before launch. There are three areas where the on-orbit behavior has required adjustments to the data analysis and mission planning procedures. Some details for the sensitivity to Solar activity, mast thermal motion, and spacecraft star tracker attitude control are given in this section.

8.1 Solar Activity

The sensitivity of the *NuSTAR* instrument background to Solar activity is higher then expected from pre-launch modeling and has required development of additional screening criteria in data processing. The screening of detector events around SAA passage is identified by comparing the high gain instrument shield event rates to increases in CZT detector countrates. Figure 22 shows the level of detector background event rates as the spacecraft orbits the Earth. The top panel illustrates the stability of background event rates (< 1 cts/s) for periods with no Solar activity. The increase in observed shield and detector background event rates is correlated with the global level of geomagnetic activity, parameterized as K_p *index*, often triggered by coronal mass ejections from the Sun.

Observations performed during periods when K_p >~ 4 show increased background event rates at ground trace positions close to the SAA. The NuSTARDAS parameter *saamode = OPTIMIZED* will screen periods when an increase in both the instrument shield and detector event rates are seen. This will extend the time of SAA passage and so decrease the available exposure time but usually only by a few %. When an investigation of a science target requires very stable background rates the parameter *saamode = STRICT* may be used. This filter identifies high background periods only using the increase in shield event rates. This conservative screening may remove 10% of the available exposure time. The example in the middle panel of Figure 23 shows the spatial effect of the different SAA filter modes for an observation on 2014-05-05 where the geomagnetic activity index rose to Kp = 4.

Investigation of the time variation of *NuSTAR* instrument background rates also identified a North-West spur to the SAA that was called "The Tentacle". Removal of these intervals is performed within NuSTARDAS by monitoring the increase in detector background event rates as the spacecraft is entering the SAA (i.e. when the ground trace latitude is 270° < Lat < 350° deg). The NuSTARDAS parameter *tentacle = yes* will filter these periods of higher background, sometimes removing 10% of available exposure time. The example on the lower panels of Figure 23 is from an observation on 2013-10-08 when the geomagnetic activity index rose to K_p = 5 (NOAA space weather geomagnetic storm level G1).

The algorithm for these SAA related filters has been verified for observations of steady sources with fluxes not dominating over the detector background. This screening is most useful for *NuSTAR* survey programs and investigations of the variability of faint sources.

The algorithm for these SAA related filters has been verified for observations of steady sources with fluxes not dominating over the detector background. This screening is most useful for *NuSTAR* survey programs and investigations of the variability of faint sources.
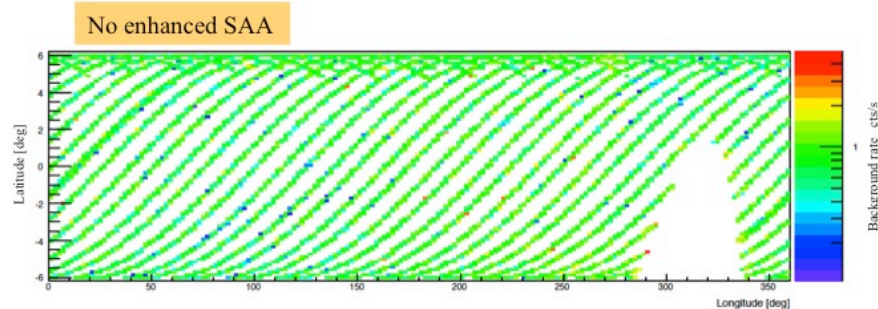

Figure 22 *NuSTAR* ground trace plot for GTI (target unocculted by the Earth and not in SAA) with the backound event rate color coded. The North tip of the SAA is the region between longitudes 280° < Lon < 350° and latitude -6° < Lat < +2°. This illustrates the background stability for observation during a period with no major Solar activity. The *NuSTAR* orbit is prograde (West to East, blue arrow) with the orbital plane recession rate of -7.22° / day (i.e. East to West, black arrow).
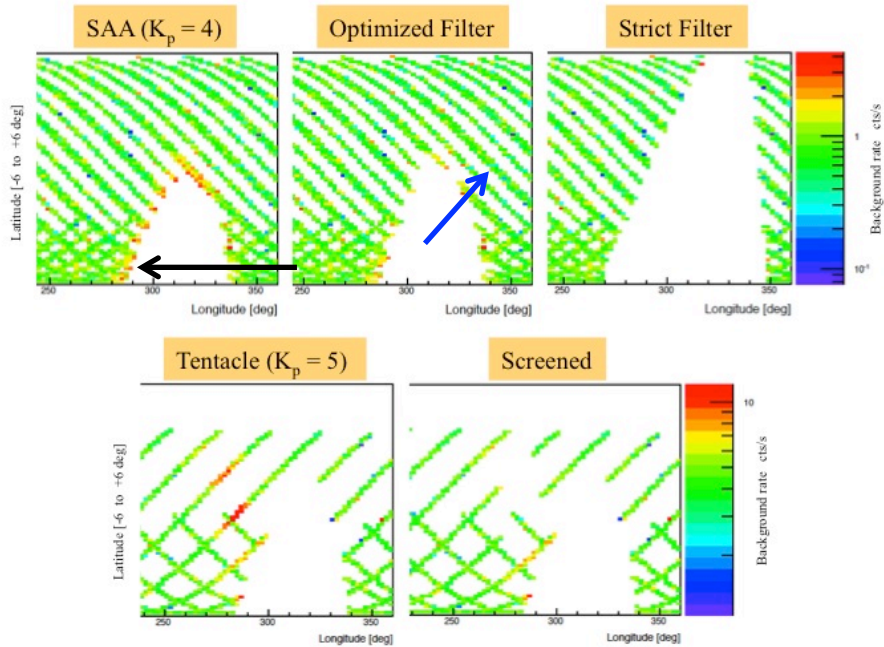
Figure 23 *NuSTAR* ground trace plots for GTI with the backound event rate color coded. *Top* – Increased detector background when spacecraft is close to the SAA during a K_p = 4 event, and the effect of available screening options. *Lower* – Increased detector background (tentacle) during a minor geomagnetic storm (K_p = 5) and the effect of screening.

Another soft X-ray component to the *NuSTAR* instrument background is clearly related to Solar activity and only present when the spacecraft is in sunlight. *NuSTAR* does not observe closer then 50 degrees to the Sun during normal operations, but the detectors often register rapid increase in background events during Solar X-ray flares. These Solar X-rays must be scattered from various elements on the spacecraft (mast, aperture stops, optics bench) onto the focal plane.
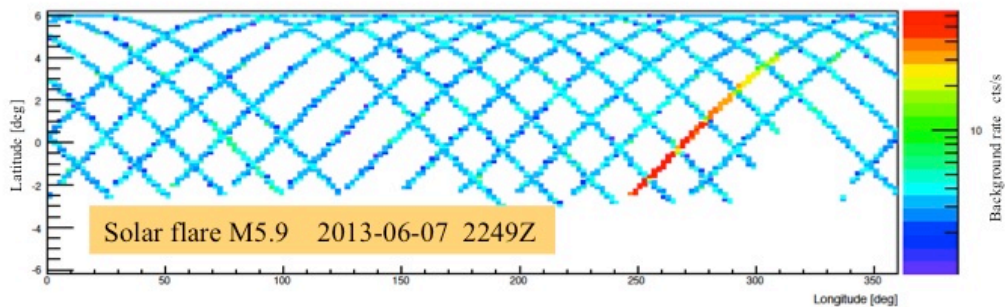

Figure 24 Increased detector background during Solar X-ray flare.

There is no automated screening in NuSTARDAS for these Solar flare events and users must manually set the GTI for the observation to exclude the time around the event.

8.2 Mast Thermal Motion

The mast provides the required 10.14m separation between the optics and focal plane bench was designed to minimize thermal flexing of the structure. The mast motion is tracked using the laser metrology system which provides 0.1″ accuracy to the determined location of the optical axis on the focal plane. Detailed simulations before launch indicated that the relative motion of the optical axis (OA) of the mirror assembly would be on average 3 mm (1′) across the focal plane detectors. The motion of the optical axis is centered on different locations on the detectors that depend on the angle of illumination of the spacecraft by sunlight (Solar aspect angle, or Saa). This was verified with a series of observations across the sky during the first 2 weeks of performance verification operations, the character and magnitude of the OA motion is almost exactly as modeled before launch.
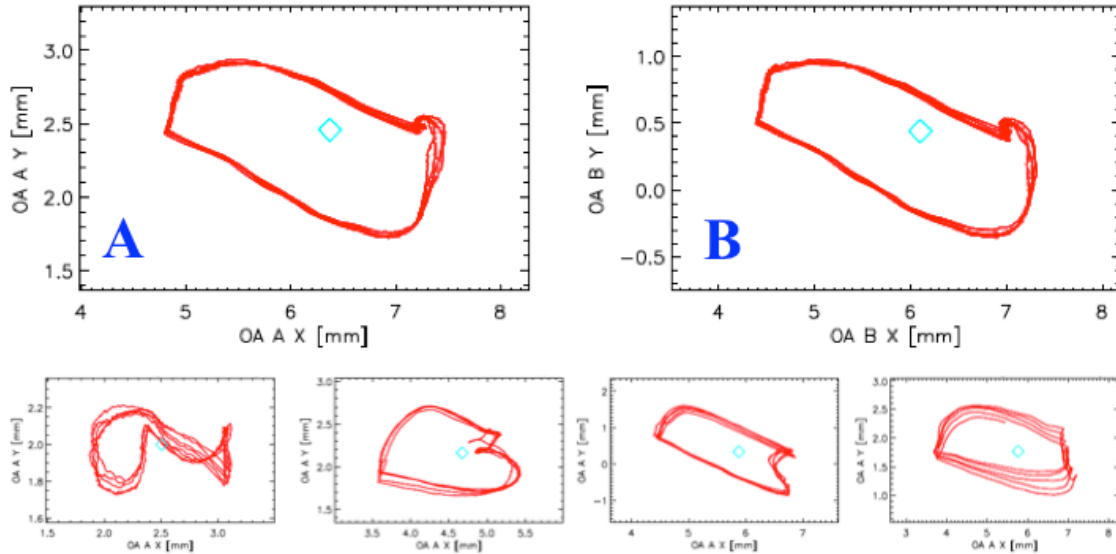

Figure 25 Motion of the optical axis (OA) across the focal plane during an observation. Top: Motion of the OA on FPMA (*left*) and FPMB (*right*) for an observation at Saa 120 deg. Lower: Motion of the OA on FPMA for observations at Saa 51, 83, 124, 170 degrees (*left to right*).

The sky position of the optical axis as a function of time is determined in NuSTARDAS using the metrology data and this is then used to calculate the time dependent off-axis angle of a given celestial source and hence the effective area correction factor for the observation.

The location of the center of motion of the optical axis can be refined using the mast adjustment mechanism (MAM) and the optimal location away from the gaps between the detectors and within the calibrated range on the laser metrology system was determined during observatory performance verification. This nominal position is located on DET0 in each focal plane assembly (see Figure 20). For most observations the location of the OA is closer to the detector gaps then the width of the instrument PSF and so most targets are placed a few mm from the optical axis as a compromise between the loss of photons falling in the detector gaps and the lower off-axis effective area away from the position of the OA.

The equilibrium alignment of the mast is expected to change very gradually with time, so that occasional adjustment of the telescope alignment is required. During 2013 there was an increase in the number of observations with a mast motion that moved the laser metrology across the edge of the calibrated area of the metrology system. These periods of uncalibrated mast motion are automatically removed from the GTI by standard processing with NuSTARDAS, although there is an option to allow these periods to be retained in data analysis, with a loss of OA positional accuracy, which has minimal impact on the analysis of bright sources. An adjustment to the telescope alignment was performed using the MAM on 2013-09-17 which moved the optical axis location 2mm on the focal plane. Subsequent observations at all Saa have kept the laser metrology system within the calibrated range
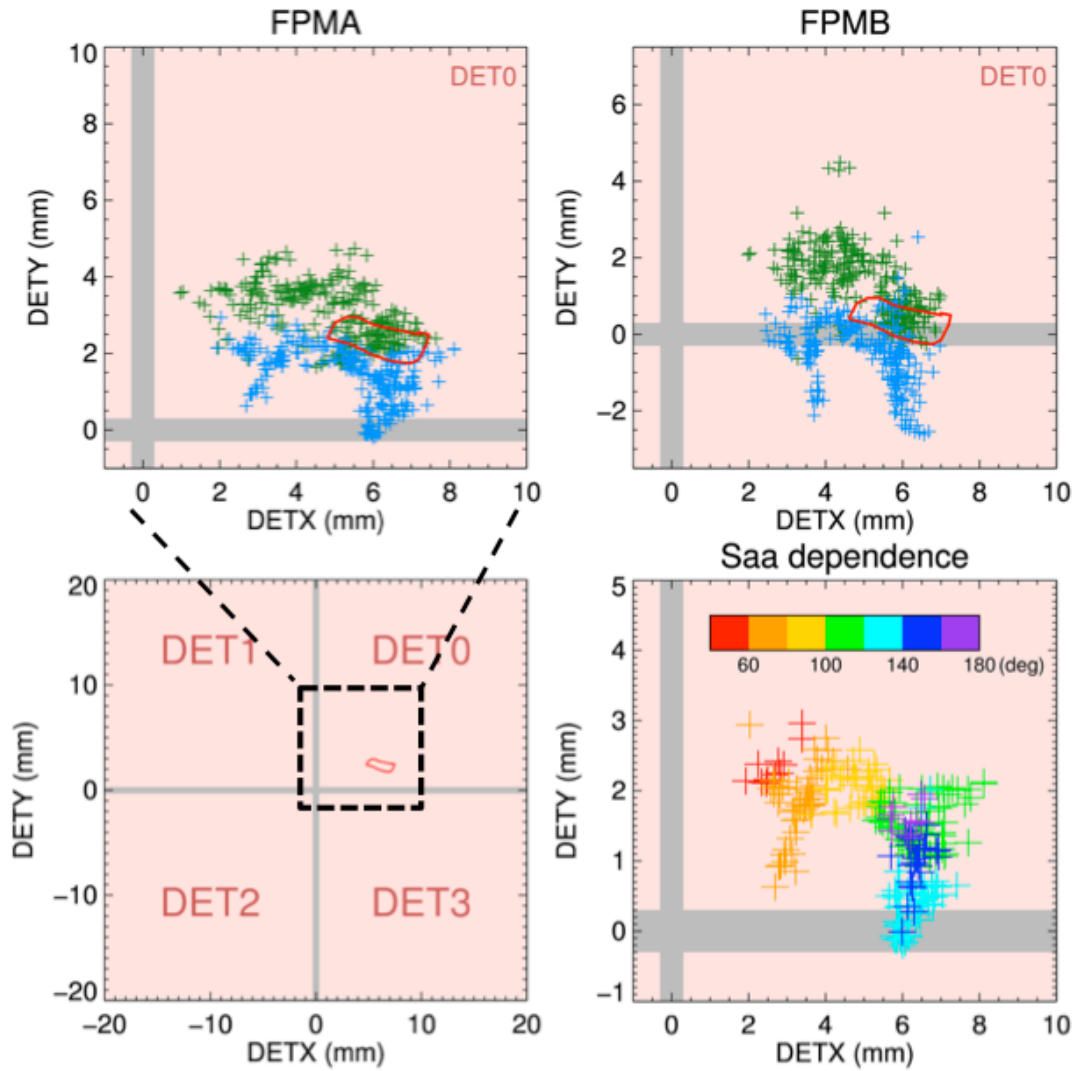
Figure 26 Mean position of the telescope optical axis (OA) motion on the focal plane detectors. Lower-Left: Arrangement of the four CZT detectors in each focal plane module. The 0.6mm gaps between the CZT detectors is shown in gray. A typical motion of the OA during an observation is 3mm (red oval on DET0). *Top-Left* - Centroid of the motion of the OA on FPMA for each observation before (green) and after (blue) the OA adjustment on 2013-09-17. A sample motion of the OA during one observation is shown in red. The character of the motion changes with differing thermal conditions (see Figure 25). *Top-Right* - The OA position on FPMB. The twisting of the mast with differing thermal conditions results in the difference in the OA position between the two telescopes. *Lower-Right* - FPMA OA position for observations after 2013-09-17. The color coding represents the average Solar aspect angle (Saa) during each observation.

8.3 Attitude Pointing Stability

One of the primary challenges of the early mission was managing the changing alignment of the star trackers with pointing direction, which can cause changes in pointing and potentially place targets in sub-optimal locations on the focal plane. There are multiple elements to each calculation of the commanded attitude of the spacecraft to place the target at the desired location on the focal plane.

1. Offset between spacecraft Z-axis alignment and telescope boresight.
2. Dependence of spacecraft ACS solution with solar illumination of spacecraft.
3. Relative offsets between ACS solution from various combinations of attitude solution from the three spacecraft startrackers.
4. Expected centroid of OA motion on focal plane and the relative importance of high energy (E > 30 keV) event signal to noise ratio.

The primary constraint on the spacecraft attitude is the requirement to keep the Sun on the side of the observatory where the solar array is located. Pointing at a celestial target thus involves a rotation of the spacecraft about the Sun-Earth vector with a small margin to keep the Sun within +2 to -10 degrees normal to the solar array. So for any particular target the position angle for the observation is determined by the date of the observation (see section 7).

(1) It was recognized early during the performance verification phase that the commanded sky position did not place the target in the field of view of the instrument. Initially it was thought that this could be FIXEDword by the planned alignment calibration of the spacecraft +Z axis and telescope boresight. However, the magnitude and direction of the relative alignment is dependent on the Solar aspect angle (Saa) during the observation and it was not possible to adjust the spacecraft flight software to enable on-board offset coordinate solutions.

Instead, the SOC calculates an offset pointing coordinate based on the J2000 coordinates of the target, the position angle for the observation (determined by the date of the observation), and the desired location of the target on the focal plane. Offset pointing coordinates are usually within 46 – 48 arcmin of the J2000 target coordinates and the commanded inertial attitude quaternion is calculated based on these offset coordinates.

(2) The nominal desired location of the target on the focal plane is on the DET0 detector at [X,Y] = [+4.0,+4.0], this keeps the target away from the gaps between the detectors and close enough to the expected location of the optical axis. However, the complex Solar illumination and shadowing of the three spacecraft star trackers (called Camera Head Units or CHU), and the thermal flexing of the spacecraft components they are mounted to, changes the alignment of each CHU and results in an additional uncertainty in the attitude solution.

This additional correction is determined from inspection of the focal plane locations if targets in recent observations, within ~40 days and ~50 degrees of the planned target. The locus of this reference target coordinate on the focal plane is compared to the desired location for that observation and the aim point for the new observation is adjusted accordingly. The closer the reference target is, in time and sky coordinates, the more successful the correction. The aim point calculation for the new target also includes an aberration correction based on the observed track of the reference target coordinates across the focal plane and the great circle distance to the new target. The calculated aim point (in detector [X,Y] mm) is then used in the calculation of offset pointing coordinates.

The use of this "boot-strap" method in aim point calculations is successful in most cases but there are occasions where no good reference target is available or the spacecraft ACS does not behave in the expected manner. So the data from the first three orbits of every observation is reviewed as soon as it is downlinked and automatically processed. Plots of the track of the target coordinates on the focal plane, based on the attitude solution from star tracker on the optics bench (CHU4) are used to determine if a small refinement in the attitude would improve the quality of the observation. The small number of ground stations passes each day limits the opportunity to perform these corrections to observations that are at least one day long, in general it is not worth performing the adjustment if there is less then half the scheduled observation remaining. An example of an aim point refinement is given in Figure 27 below.
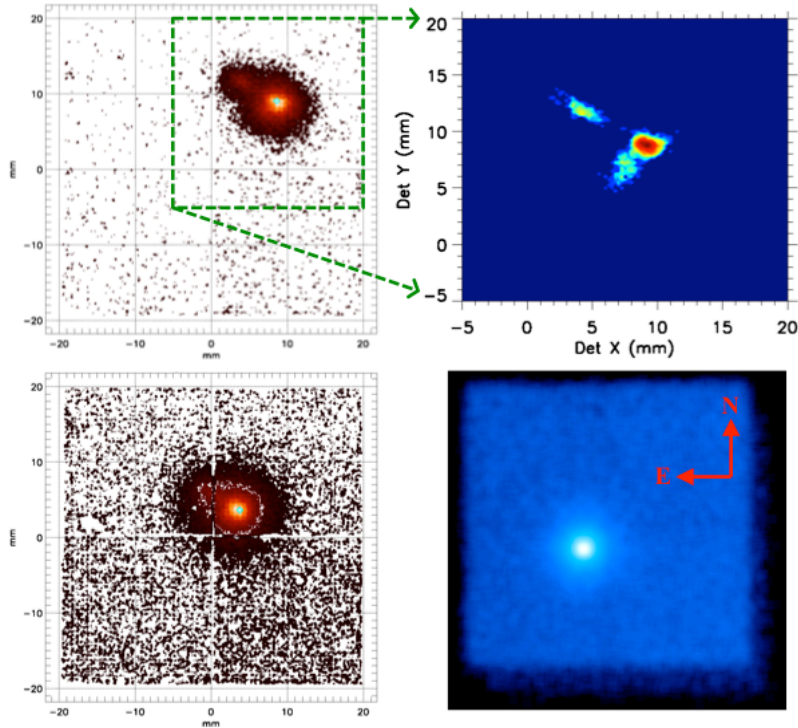
Figure 27 X-ray event image (FPMA) in detector coordinates from an observation of Fairall 9 on 2014-05-09. *Top Left –* Image from initial 49 ksec exposure with an offset coordinate calculation based on estimated aim point. *Lower Left –* Final 94 ksec of the observation after an aim point refinement of Δ[X,Y] = [-5,-5]. *Top Right* - Contour image of location of target coordinates on focal plane before aim point refinement. *Lower Right –* Reconstructed sky image for the observation (PA 89° deg) after the aim point refinement, North is up and East is to the left. Detector +X direction is down and +Y direction is to the left.

Review of the first few orbits of data from the observation of the active galaxy Fairall 9 in May 2014 (ObsID 60001130002) indicated that the target was more then 2 arcmin from the optimal location on the detectors (see Figure 27). So a new offset coordinate was calculated from an adjustment to the aim point on the focal plane of Δ[X,Y] = [-5,-5] mm and uploaded to the spacecraft within a day of the beginning of the 2.5 day observation. The locus of the optical axis motion during this observation was at $[X_{OA},Y_{OA}] = [+3.8, +2.3]$ mm and the aim point refinement placed the centroid of the target coordinates at [X,Y] = [+4,+4]. The aim point refinement improved the S/N of the observation, particularly above 30 keV. An aim point closer to the position of the optical axis (which does not change with pointing refinements) would result in events in the wings of the PSF (HPD ≈ 3mm) falling into the detector gaps.

(3) The spacecraft attitude control system (ACS) combines the attitude solution of the three CHU (1,2,3) on the spacecraft bus and is designed to actively control the attitude to within 1 arcsec during an observation, performing adjustments to keep the spacecraft +Z axis oriented towards the science target. At least on CHU must be unblocked by the Earth, Sun, or Moon at any time to provide an attitude solution. A fourth star tracker mounted on the optics bench and co-aligned with the X-ray optics provides absolute astrometry for every observation. Observations taken during performance verification showed that the field of view of the telescope was moving across the sky by up to 5 arcmin during some exposures even though the spacecraft attitude solution was nominal.

An example of this additional motion is shown in Figure 28 below for the observation of Fairall 9 shown in Figure 27 above. The target position on the focal plane is determined from the CHU4 astrometry solution which is unavailable when the camera field of view is occulted by the Earth. The track of the target position is expected to have a motion similar to the OA track due to thermal flexing of the mast, of order 3mm in extent.
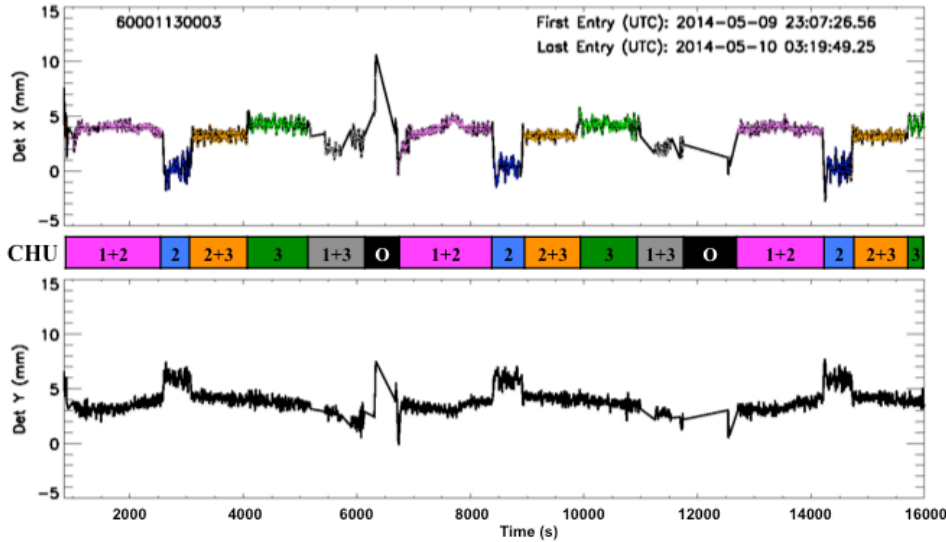
Figure 28 Motion of target position on focal plane for three orbits of observation of Fairall 9 on 2014-05-09 at Saa = 79 deg (ObsID 60001130002). *Top* – Motion in detector X direction. *Lower* – Motion in detector Y direction. *Middle* – Progression of valid attitude solutions from CHU 1,2,3 that drive the spacecraft ACS.

No absolute astrometry is available during the short periods when CHU4 occulted by the Earth (O). The pattern of CHU combinations driving the spacecraft attitude solution repeats each orbit as the CHUs become occulted by the Earth. The top-right panel of Figure 27 shows a contour image of this motion for the entire exposure.

The complex shadowing and illumination by the Sun of the locations where the CHU are mounted changes the alignment of the CHU in a way not accounted for in the on-board CHU alignment calibration matracies and flight software. The combination of attitude information from the CHUs fed into the ACS changes as the CHU field of view become occulted by the Earth during each orbit. Figure 28 above shows how the combination of various CHU contributing to the ACS changes the absolute astrometry during three orbits of an observation. The ACS will perform small adjustments to the spacecraft attitude to keep the spacecraft at the "correct" attitude. This pattern is repeated throughout the observation, only slowly changing as the *NuSTAR* orbit precesses and the occultation timing for the CHUs changes.

The impact of this additional motion on the scientific quality of most observations is minimal because 90% of the total ontarget time for observations at almost all Saa places targets within ±1.5 mm (30″) of the centroid of the motion. The only other impact is an operational recommendation to keep the yaw-offset as close to -5 degrees as possible to avoid glints from the Sun effecting the performance of CHU3. The PA for almost all observations is chosen to have a yaw-offset at -5 degrees in the middle of the scheduled observation. Figure 29 shows a contour image of the relative motion of the target position on the focal plane taken from over 800 observations ($>3x10^6$ measurements) during the first two years of the mission. The relative positions are normalized with the centroids for each observation placed at [6,6]. The plot has a logarithmic scale with 90% of all target position measurements in the red area.
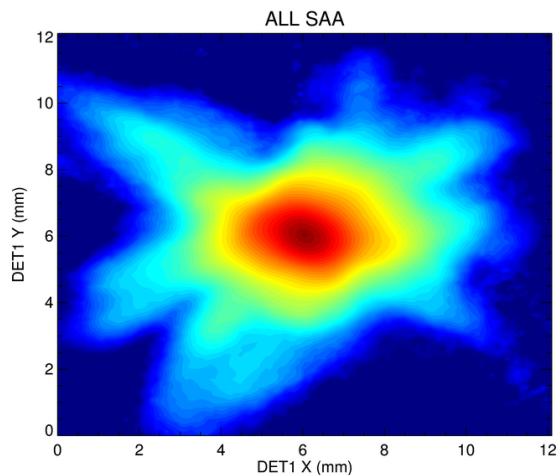
Figure 29 Contour image of target positions on the focal plane normalized to the centroid of the motion in each observation (placed at [6,6]). The contour has a logarithmic scale to show the extent of the relative motion. 90% of the total ontarget time for the mission has target positions within ±1.5 mm (30″; red area) of the centroid of the motion.

This motion is fully calibrated during data processing including changes in detector response at the location of each X-ray event and the adjustment in effective area due to off-axis angle. There are differences in the detailed pattern of this motion dependent on the Saa during the observation, and this can be detrimental if detailed timing analysis is being performed and the ACS adjustment moves a detector gap over the source, however the impact on the aim point calculation of this motion is not usually taken into account because the magnitude of the motion is of order the same as the uncertainty in the aim point calculation.

9. MISSION OPERATIONS

NuSTAR operations is a collaboration between the Science Operations Center (SOC), in the Cahill center for astronomy and astrophysics at the California Institute of Technology (Caltech), Pasadena CA, and the Mission Operations Center (MOC) managed by the UC Berkeley Space Sciences Laboratory (SSL), Berkeley CA[11].

The *NuSTAR* SOC performs all science planning and data processing functions and monitors the health of the instrument and telescope. This includes survey and observation planning, observatory scheduling, and monitoring survey progress to maximize the scientific return from the mission. Automated data processing is performed daily at the SOC and includes monitoring the data quality and the validation of science processing. The SOC leads observatory calibration activities, including ground based and in-orbit measurements, and delivers calibrated data products to the *NuSTAR* science team and the public through the High Energy Astrophysics Archive (HEASARC) at the Goddard Space Flight Center. Data processing software has been developed at the SOC in collaboration with software engineers at the ASI Science Data Center (ASDC, Italy).

9.1 Attitude Control During Observations

The slewing of the observatory to point the telescope at the celestial position of a new science target is performed in two stages:

1. A preliminary long (average 20 minute ~ 70°) slew in STELLAR ACS mode that orients the spacecraft to point the observatory at a target position on the celestial sphere and with an orientation that keeps one side of the observatory facing the Sun.

2. A second slew, usually < 5°, to set the observatory in an INERTIAL attitude for the duration of the science observation. This slew is timed to begin at least 5 minutes after the completion of the STELLAR mode slew to allow settling of the spacecraft attitude between slews.

STELLAR ACS mode is unsuitable for long science observations because it includes a slow roll about the telescope boresight axis to keep the Sun at a fixed angle with respect to the solar panels. This will cause the field of view of the telescope to move across the sky, so an INERTIAL attitude is used during science observations. The fixed attitude in INERTIAL ACS mode is calculated to keep the Sun within 5 degrees of the nominal angle to the solar panels and so is generally acceptable for observations lasting up to a week.

The timing of these slews is calculated so that the slew maneuvers and settling will complete while the new science target is occulted by the Earth.

Exceptions to the standard observation modes and slew timing include:

I. Target of opportunity observations that require arrival at the new target as soon as possible.

II. Survey observations are performed by overlapping the field of view in regions only a few degrees across. No STELLAR mode slew is required between these positions when observed concurrently so only INERTIAL mode slews are executed.

III. Observations of targets at high Declination, |Dec| > 65°, may be observed at times when the target is not occulted by the Earth each orbit, so the STELLAR mode slew is timed to begin soon after entry into Earth occultation of the previous target to maximize efficiency.

9.2 Ground Station Support

Ground station support scheduling is based on the expected data volume for the targets tabulated in the 9 day ATS. Standard operations support uses four 10-minute contacts per day through the Italian Space Agency's (ASI) Malindi ground station in Kenya. This provides approximately 100% margin for data recovery during nominal science operations. On-board storage of X-ray event data is limited to 2.8 Gbit and the median brightness of science targets observed during the primary mission induces a data rate of 15 kbit/s.

Additional ground station passes are scheduled to support the higher data volume observations of bright X-ray sources, like the Crab nebula, using Kongsberg Satellite Services antenna in Singapore and Universal Space Network's antennas at South Point, Hawaii, with sometimes as many 15 contacts/day.

9.3 Data Processing

NuSTAR science data and engineering housekeeping are processed automatically at the SOC upon receipt of raw data files from the MOC, using information in the *NuSTAR* As-Flown Timeline log (AFT). The AFT is a time ordered list of the sequence of *NuSTAR* observations starting from launch (and eventually ending at spacecraft decommissioning. This table is available on the *NuSTAR* SOC and HEASARC websites and is updated weekly.

http://www.srl.caltech.edu/NuSTAR_Public/NuSTAROperationSite/AFT_Public.php

http://heasarc.gsfc.nasa.gov/W3Browse/nustar/nuaftl.html

One *NuSTAR* observation is defined as an "un-interrupted" look at the same sky position. Each observation is assigned a unique observation ID (ObsID), to identify the data taken within that interval of time. A new ObsID is assigned every time the satellite slews to a different position in the sky with the slew period preceding the start of an observation kept within that observation. An observation is associated to any time during satellite operations and an ObsID tags every observation. The ObsID is an 11 digit sequence, the first 8 digits are governed by information in the SOC mission planning system (MPS) and the final 3 digits are a sequential visit number for the target. The majority of *NuSTAR* observations will contain two ObsIDs; the first containing the STELLAR mode slew from the previous target, and the second the science observation in INERTIAL mode.

Every observation is examined in detail at the SOC using a quality assurance (QA) system developed to display instrument telemetry trending, detector images, spacecraft attitude stability, and also detector background measurements used to determine the impact of Solar activity on the quality of each observation (see section 8.1). The SOC QA system is also used to examine the pointing accuracy based on the first few orbits of data for each observation. If the science target is not in the optimal position on the detectors a correction to the spacecraft attitude may be calculated by the SOC and a new ATS generated for upload on the next available contact. Data associated with this attitude refinement will be contained in a new ObsID but the science data from all ObsID's associated with a target can be co-added or analyzed together; one of the benefits of using photon counting detectors.

REFERENCES

[1] Harrison, F.A., Craig, W.W., Cristensen, F.E. et al., "The Nuclear Spectroscopic Telescope Array (*NuSTAR*) High-Energy X-ray Mission", The Astrophysical Journal, 770, 103 (2013).

[2] Madsen, K.K. et al. "*NuSTAR* in-orbit calibration", in preparation (2014)

[3] Jorgensen, P.S., Jorgensen, J.L., and Denver, T., in "Proceedings of the 4S Symposium: Small Satellites, Systems and Services" Ed. B. Warmbein, v571 (ESA SP-571) (2004).

[4] Farr, T.G. et al., "The Shuttle Radar Topography Mission", Reviews of Geophysics, 45, 2004 (June 2007).

[5] Petre, R. and Serlemitos, P., "Conical Imaging Mirrors for High-Speed X-ray Telescopes", Applied Optics 24 1833 (1985).

[6] Koglin, J. E. et al., "*NuSTAR* hard x-ray optics design and performance", Society of Photo-Optical Instrumentation Engineers (SPIE) Conference Series 7437 (2009).

[7] Madsen, K. et al., "Optimizations of Pt/SiC and W/Si multilayers for the Nuclear Spectroscopic Telescope Array", Society of Photo-Optical Instrumentation Engineers (SPIE) Conference Series 7437 (2009).

[8] Christensen, F. E. et al., "Coatings for the *NuSTAR* mission", Society of Photo-Optical Instrumentation Engineers (SPIE) Conference Series 8147 (2011).

[9] Kitaguchi, T. et al., "Spectral calibration and modeling of the *NuSTAR* CdZnTe pixel detectors", Society of Photo-Optical Instrumentation Engineers (SPIE) Conference Series 8145 (2011).

[10] Kitaguchi, T. et al., "Inflight performance and calibration of the *NuSTAR* CdZnTe pixel detectors", Society of Photo-Optical Instrumentation Engineers (SPIE) Conference Series 9144 (2014).

[11] Roberts, B. et al., "Highly automated on-orbit operations of the *NuSTAR* telescope", Society of Photo-Optical Instrumentation Engineers (SPIE) Conference Series 9149 (2014).

[12] Baumgartner, W.H. et al., "The 70 Month *Swift*-BAT All-sky Hard X-ray Survey", The Astrophysical Journal Supplement, 207, 19 (2013).

[13] Wik, D.R. et al., "NuSTAR observations of the Bullet cluster: Constraints on Inverse Compton Emission", ApJ in press (arXiv: 1403.2722) (2014)

[14] Sembay, S. et al., "Defining High-Energy Calibration Standards: IACHEC (International Astronomical Consortium for High-Energy Calibration)" in "X-ray Astronomy 2009: Present status, multi-wavelength approach and future perspectives" AIP conference proceedings, 1248 593 (2010). URL: http://web.mit.edu/iachec/index.html (2014)

[15] Arnaud, K.A. "XSPEC: The First Ten Years" in "Astronomical Data Analysis Software and Systems V", Eds G.H. Jacoby and J. Barnes, A.S.P. Conference series, 101, 17 (1996).

[16] Pence, W. "NASA office of guest investigator programs (OGIP) FITS format recommendations", URL: http://heasarc.gsfc.nasa.gov/docs/heasarc/ofwg/ofwg_intro.html (2011).

[17] Pence, W. "FITSIO, v2.0: A New Full-Featured Data Interface" in ASP Conf. Ser. Vol. 172. Astronomical Data Analysis Software and Systems VIII, ed. D.Mehringer, R. Plante, and D. Roberts (San Francisco: ASP), 487 (1999).

[18] Arnaud, K.A. and Dorman, B. "XANADU: Data analysis for X-ray Astronomy" URL: http://heasarc.gsfc.nasa.gov/lheasoft/xanadu/ (2013).

[19] NASA/IPAC Infrared Science Archive (IRSA). URL: http://irsa.ipac.caltech.edu/frontpage/ (2014).

[20] The Barbara A. Mikulski Archive for Space Telescopes (MAST), URL: https://archive.stsci.edu (2014).

[21] Perry B. and Johnson M. "Data Transfer System (DTS) User's Guide", URL: http://heasarc.gsfc.nasa.gov/dts/ (2004)